



# Mid-Miocene to Present Upper-Plate Deformation of the Southern Cascadia Forearc: Effects of the Superposition of Subduction and Transform Tectonics

Kirsty A. McKenzie<sup>1\*</sup>, Kevin P. Furlong<sup>1</sup> and Eric Kirby<sup>2</sup>

<sup>1</sup>Department of Geosciences, The Pennsylvania State University, University Park, PA, United States, <sup>2</sup>Department of Earth, Marine and Environmental Sciences, The University of North Carolina, Chapel Hill, NC, United States

## OPEN ACCESS

### Edited by:

Juan Díaz-Alvarado,  
Instituto Geológico y Minero de  
España (IGME), Spain

### Reviewed by:

Antonio Pedrera,  
Instituto Geológico y Minero de  
España (IGME), Spain  
Andrés Folguera,  
University of Buenos Aires, Argentina

### \*Correspondence:

Kirsty A. McKenzie  
kam724@psu.edu

### Specialty section:

This article was submitted to  
Structural Geology and Tectonics,  
a section of the journal  
Frontiers in Earth Science

**Received:** 09 December 2021

**Accepted:** 10 January 2022

**Published:** 07 February 2022

### Citation:

McKenzie KA, Furlong KP and Kirby E  
(2022) Mid-Miocene to Present Upper-  
Plate Deformation of the Southern  
Cascadia Forearc: Effects of the  
Superposition of Subduction and  
Transform Tectonics.  
Front. Earth Sci. 10:832515.  
doi: 10.3389/feart.2022.832515

The southern Cascadia forearc undergoes a three-stage tectonic evolution, each stage involving different combinations of tectonic drivers, that produce differences in the upper-plate deformation style. These drivers include subduction, the northward migration of the Mendocino triple junction and associated thickening and thinning related to the Mendocino Crustal Conveyor (MCC) effect, and the NNW translation of the Sierra Nevada-Great Valley (SNGV) block. We combine geodetic data, plate reconstructions, seismic tomography and topographic observations to determine how the southern Cascadia upper plate is deforming in response to the combined effects of subduction and NNW-directed (MCC- and SNGV-related) tectonic processes. The location of the terrane boundaries between the relatively weak Franciscan complex and the stronger Klamath Mountain province (KMP) and SNGV block has been a key control on the style of upper-plate deformation in the southern Cascadia forearc since the mid-Miocene. At ~15 Ma, present-day southern Cascadia was in central Cascadia and deformation there was principally controlled by subduction processes. Since ~5 Ma, this region of the Cascadia upper plate, where the KMP lies inboard of the Franciscan complex, has been deforming in response to both subduction and MCC- and SNGV-related effects. GPS data show that the KMP is currently moving to the NNW at ~8–12 mm/yr with little internal deformation, largely in response to the northward push of the SNGV block at its southern boundary. In contrast, the Franciscan complex is accommodating high NNW-directed and NE-directed shortening strain produced by MCC-related shortening and subduction coupling respectively. This composite tectonic regime can explain the style of faulting within and west of the KMP. Associated with this Mendocino Crustal Conveyor crustal thickening, seismic tomography imagery shows a region of low velocity material that we interpret to represent crustal flow and injection of Franciscan crust into the KMP at intracrustal levels. We suggest that this MCC-related crustal flow and injection of material into the KMP is a relatively young feature (post ~5 Ma) and is driving a rejuvenated period of rock uplift within the KMP. This scenario provides a potential explanation for steep channels and high relief, suggestive of rapid erosion rates within the interior of the KMP.

**Keywords:** tomography, GPS, subduction, cascadia, triple junction, forearc

## INTRODUCTION

Upper-plate deformation in subduction zone forearcs occurs in response to both short-term (earthquake cycle) and long-term (million-year plate interaction) processes. New observations of present-day and long-term upper-plate deformation along subduction zones globally allow us to identify both upper-plate behavior that is common across subduction zones as well as differences in the deformational response of the upper plate among different subduction margins. For example, during the 2016 Kaikoura, New Zealand event, slip on upper-plate faults was significant (~5–10 m) and was coincident with slip on the Hikurangi subduction megathrust (Furlong and Herman, 2017; Wang et al., 2018). Additionally there was 0.6–4.8 m of uplift of the coastline during this event (Hamling et al., 2017). Similar upper-plate faults exist in subduction zones globally and understanding the tectonic processes that load these faults and when they slip during the seismic cycle is important for assessing hazard across subduction forearcs. Although the Cascadia subduction zone has not experienced a major megathrust earthquake in modern times, and as a result we do not have direct observations of its rupture behavior, detailed recording of its current behavior by geodetic methods, and constraints on its plate tectonic evolution make it an ideal plate boundary to explore how plate interactions and the evolution of a plate boundary over millions of years produces permanent deformation of the upper plate.

The Cascadia subduction zone extends along the western coast of North America from northern California to British Columbia (Figure 1) and is defined by the position of the Mendocino triple junction (MTJ) at its south end and a triple junction at its north end where the Nootka Fault Zone (NFZ) links the northern end of the Juan de Fuca ridge to the Cascadia subduction zone (Rohr et al., 2018). The MTJ migrates northward along the western margin of North America at approximately 50 mm/yr (Furlong and Schwartz, 2004), while the northern triple junction has been relatively stationary with respect to North America since ~4 Ma (Rohr et al., 2018). As a result, the length of the Cascadia subduction zone has systematically shortened over time (Figures 1, 2). Thus, the plate tectonic setting of our study area in southern Cascadia has significantly changed since the mid-Miocene (~15 Ma), at which time it was centrally located along the plate boundary, as compared to its current location adjacent to the MTJ (Figure 2).

This change in the geography of southern Cascadia over the last 15 million years, and the associated changes in tectonic interactions in the region lead to a suite of tectonic processes (subduction and transcurrent tectonics) that have contributed at different times and in different ways to upper-plate deformation in the region. These tectonic drivers act on a spatially varying upper-plate geology (Figure 1) resulting in distinctive styles of upper-plate deformation in both space and time. Here we explore how the upper-plate geology, subduction-interface earthquake-cycle coupling, and non-subduction tectonic processes associated with the northward encroachment of the MTJ (including the development of the San Andreas plate boundary to the south) interact and produce the observed upper-plate deformation in

present-day southern Cascadia from the mid-Miocene to the present. Specifically we focus on 1) how the behavior of upper-plate faults changes as the plate boundary evolves, including the development of shear zones in the vicinity of the MTJ, and 2) the spatiotemporal patterns of uplift across different regions of the southern Cascadia forearc, including a possible rejuvenation in uplift of the Klamath Mountain province (KMP) over the last 5 million years. We address these key points by building on our recent results delineating the kinematics and strain within the terranes in the vicinity of the MTJ, including the Franciscan, Klamath, Siletz, and Sierra Nevada/Great Valley terranes (McKenzie and Furlong, 2021; McKenzie et al., 2022). We add to those results newly obtained crustal (local earthquake) tomography of the coastal region extending from north of the San Francisco Bay region to approximately 42°N (Furlong et al., 2021). This tomography provides a 3-D image of the crustal structure of the Franciscan and Klamath terranes and defines the extent of the subducting Gorda slab and the Pacific plate, south of the MTJ. We also present observations of normalized channel steepness throughout the region, which provide additional insight into which regions are potentially undergoing active uplift and exhumation.

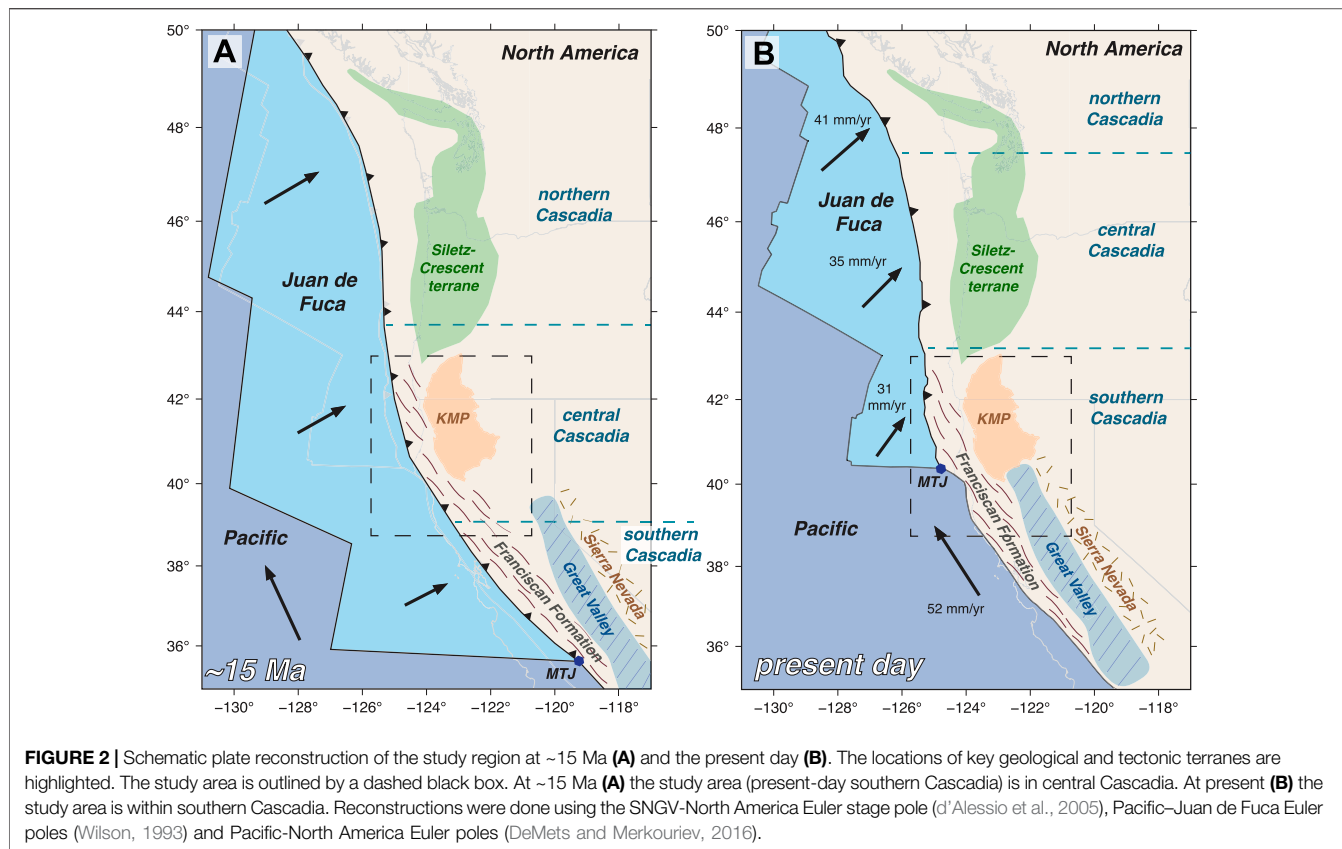
## BACKGROUND

### Geologic and Tectonic Setting

The region of southern and central Cascadia from the mid-Miocene to present-day (Figures 1, 2) includes five key geological domains: 1) the Siletz-Crescent terrane 2) the northern California Coast Ranges comprised largely of the Franciscan complex, 3) the Klamath Mountain province (KMP), 4) the Great Valley Ophiolite (mafic-ultramafic body, hereinafter referred to as the Great Valley ultramafic body) and the Great Valley Sequence, both of which are overlain by Cenozoic basin fill, and 5) the Sierra Nevada (McCroly and Wilson, 2013; Schmidt and Platt, 2018; Irwin, 1985; Godfrey et al., 1997; Ernst, 2013). North of ~43°N, the Siletz-Crescent terrane, an accreted oceanic plateau, makes up the majority of the forearc, inboard of the present-day offshore accretionary margin (Figures 1, 2) (Wells et al., 1998; McCroly and Wilson, 2013). South of ~43°N, the upper plate is composed of an active accretionary margin near the trench outboard of the Franciscan complex, a partially exhumed relict accretionary margin, which is bounded on its east by the KMP, a composite metamorphic/plutonic terrane (Irwin, 1985; Irwin, 1985; Schmidt and Platt, 2018). South of the MTJ, the Franciscan complex continues as the outboard terrane, and the KMP is replaced at ~40°N by the Sierra Nevada - Great Valley (SNGV) block composed of the accreted Great Valley ultramafic body and the Sierra Nevada terrane.

This variation in upper-plate geology and the interaction among the geologic terranes plays an important role in the style and evolution of upper-plate deformation along the western margin of North America, which can be divided into three stages, each reflecting differences in the principal tectonic drivers acting during each time period (Figures 2, 3).





*Stage 1:* When the MTJ is sufficiently south of a site, corresponding currently to the region of Cascadia north of ~43°N, the primary tectonic driver of upper-plate deformation is subduction plate interface coupling.

*Stage 2:* As the MTJ migrates northward and approaches the region of interest, NNW-directed shortening associated with the motions of the MTJ and SNGV block is superimposed on the subduction coupling signal, producing a composite deformation field.

*Stage 3:* After the MTJ passes, a slab window is created beneath the upper-plate region that experienced the previous subduction and MTJ/SNGV-related deformation. This relic upper-plate region of southern Cascadia now responds to deformation primarily within the Pacific - North America shear zone. Localization of shear and fault development within this zone leads to the development of the San Andreas plate boundary, and upper-plate deformation is overprinted on the inherited (pre-MTJ passage) structures from the prior tectonic regime.

The evolution of the plate boundaries among the Pacific, North America, and Juan de Fuca (Gorda) plates along the western margin of North America results in fundamental changes in plate interactions over millions of years. For example, the MTJ, which defines the transition from subduction to translation has migrated nearly 500 km northward, relative to North America since ~10 Ma (Atwater, 1970) (Figures 2, 3). This means that the current San Andreas plate boundary zone (Pacific - North America) north of San Francisco was part of the Cascadia subduction zone as recently as 5–10 million

years ago, with the SNGV block being the main upper-plate terrane inboard of the Franciscan complex. The San Andreas plate boundary faults have subsequently developed within a deformed upper-plate that has undergone both subduction deformation and subduction/MTJ-SNGV composite deformation prior to the passage of the MTJ.

## Development of the Present-Day Tectonic Setting

The lithospheric-scale geometry of the plate boundary in the vicinity of the MTJ results from the way in which the plate boundary changed from subduction to a system with northward and southward migrating triple junctions and the development of a transform plate boundary (Figure 3). Based on plate reconstructions the initial triple junctions formed with the interaction of a short ridge segment, bounded on its north by the intersection of the Pioneer fault with the North American margin (Figures 3A,B) (Furlong et al., 2003; Atwater, 1970). The resulting northward-migrating Pioneer triple junction (PTJ) was a short-lived configuration, and within a few million years the Mendocino fault - ridge intersection reached the trench producing the MTJ (Figure 3C). As a result, the PTJ was abandoned and the short ridge segment linking the Pioneer and Mendocino faults ceased spreading. The fragment of the Farallon plate between the two triple junctions (PTJ and MTJ), the Pioneer fragment, was captured by the Pacific plate, and has traversed the North American margin with the Pacific plate since

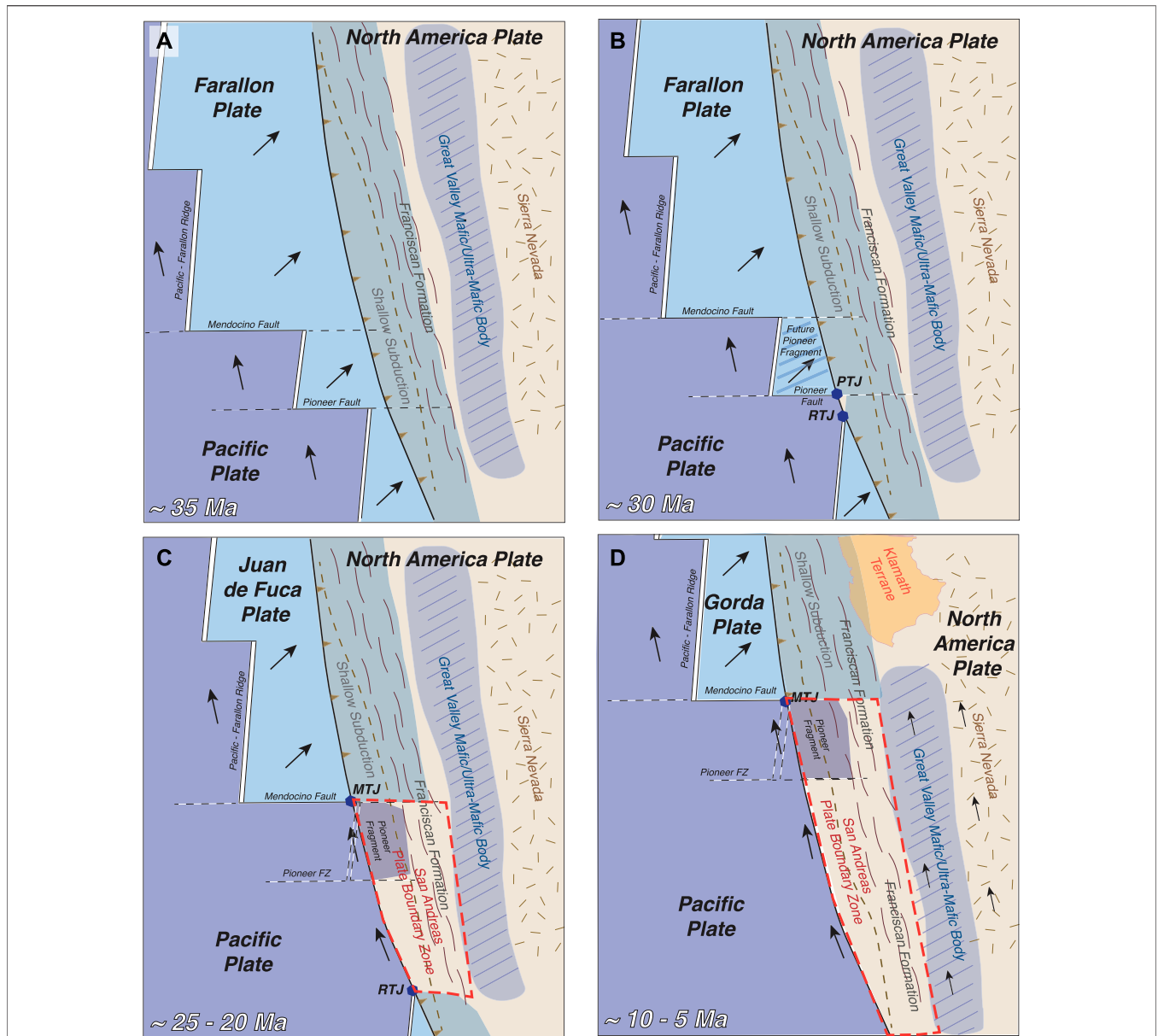


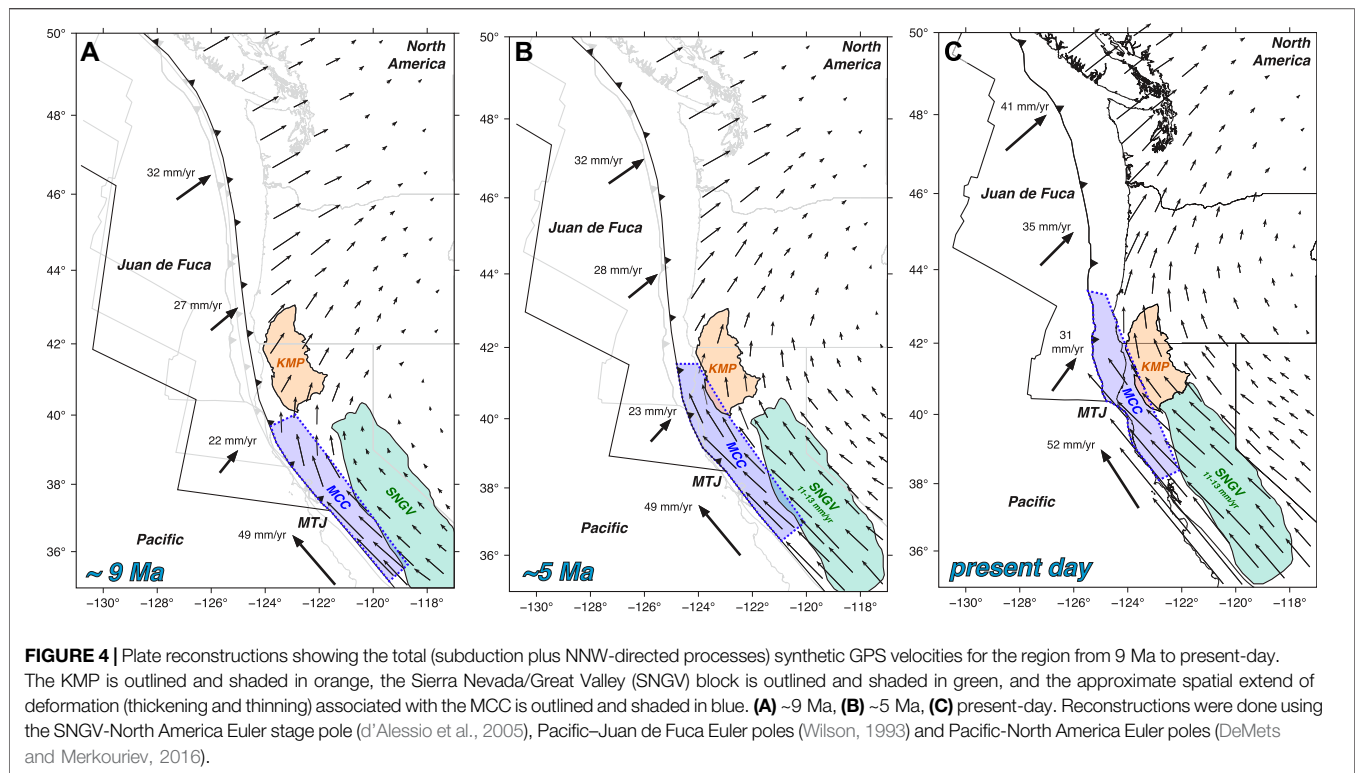
**FIGURE 3** | Schematic plate reconstruction of the region from ~35 Ma–5 Ma. The locations of key geological and tectonic terranes are highlighted. **(A)** ~35 Ma, **(B)** ~30 Ma, **(C)** ~25–20 Ma, **(D)** ~10–5 Ma.

~25 Ma as the MTJ migrates northward (**Figure 2C**) (Furlong et al., 2003). This fragment extends some distance under the western edge of North America, which results in the slab window, just to the south of the MTJ, to be narrower than might otherwise be expected, based on the subduction geometry north of the MTJ (**Figure 3D**).

### Deformational Effects of Present-Day Tectonics in Southern Cascadia

Present-day deformation in the southern Cascadia forearc is governed by the interaction of three tectonic plates, the Pacific

plate, the Juan de Fuca (Gorda) plate and the North American plate, that meet at the MTJ. With the passage of the MTJ, a slab window is created in the wake of the subducting slab (Dickinson and Snyder, 1979; Zandt and Furlong, 1982; Furlong, 1984). Furlong and Govers (1999) proposed that associated with the creation of this slab window, asthenospheric mantle will flow into the region and viscously couple the North American plate above to the adjacent southern edge of the subducting Gorda slab. This emplacement of asthenosphere into the slab window and associated viscous coupling (via the Mendocino Crustal Conveyor (MCC) model) drives a northward motion of the



overriding North American plate in the vicinity of the MTJ, leading to crustal shortening and thickening ahead of the MTJ and crustal thinning in its wake (Furlong and Govers, 1999). This wave of crustal thickening and thinning propagates to the NNW at ~50 mm/yr with the MTJ. Associated with this northward migration are variations in crustal structure, uplift/subsidence, river drainage reorganization and thermal variations within this MCC deformation corridor (Bennett et al., 2016; Lock et al., 2006; Furlong and Schwartz, 2004; Guzofski and Furlong, 2002; Beaudoin et al., 1996; Beaudoin et al., 1998). This deformation associated with the MCC (long-term NNW-oriented geologic shortening followed by extension) is superimposed in the existing subduction-driven deformational field as the MTJ approaches.

At present, in the region south of the MTJ, Pacific–North America right-lateral shear motion is accommodated in two shear zones. Approximately 75% of the motion is accommodated within the coastal region, extending to the western edge of the Great Valley (Bennett et al., 1999; Bennett et al., 2003). An additional 25% of this motion is accommodated inboard of the main plate boundary along the eastern margin of the SNGV crustal block (Bennett et al., 1999; Bennett et al., 2003), in what is termed the Eastern California Shear Zone (ECSZ). This inboard shear initiated at ~12–10 Ma, causing a change in the direction of the SNGV motion from westward to north-northwestward (McQuarrie and Wernicke, 2005). This north-northwestward motion along the northern ECSZ, and therefore motion of the SNGV block, accelerated at ~6 Ma due to the northward motion of Baja

California (Plattner et al., 2010). Taken together, this combination of tectonic processes means that present-day upper-plate deformation in southern Cascadia records the superposition of processes including Cascadia subduction earthquake cycle deformation, the migration of the MTJ and its associated thickening–thinning effects, and the NNW motion of the SNGV block facilitated by shear across the northern ECSZ (Figures 1, 4; McKenzie et al., 2022; McKenzie and Furlong, 2021).

Over the past several million years, the upper-plate region of the southern Cascadia subduction zone has undergone a transition from a subduction-only tectonic regime to a setting in which the subduction environment is becoming increasingly overprinted by deformation associated with the advancing MTJ and the SNGV block (Figures 2–4). The combination of time-varying tectonic drivers and heterogeneous upper-plate crustal properties produces a resulting deformation field that we are able to dissect in order to explore how these events and processes combine to produce the resulting geological signature of upper-plate deformation. Among the processes we identify are the localization of upper-plate shortening, active rock uplift and the development of shear zones.

## THE KINEMATIC EVOLUTION OF SOUTHERN CASCADIA

The superposition of subduction-related and NNW-directed (MTJ and SNGV) deformation can be seen in the GPS

velocity field in southern Cascadia—documented by McKenzie and Furlong (2021) (**Figure 4**, **Supplementary Figure S1**). The subduction component is driven by the earthquake cycle and so it accumulates and recovers every few hundred years during megathrust events. In contrast, the MCC- and SNGV-driven components have a characteristic time scale of a few million years and their effects are long-lived or permanent (Furlong and Govers, 1999; McKenzie and Furlong, 2021). Thus following a large megathrust earthquake, the effects of subduction zone interseismic loading of the upper plate would be largely recovered, and the residual GPS velocity field would predominantly reflect upper-plate deformation in response to the NNW-directed components.

The present-day GPS velocity field has alternatively been interpreted to reflect rotation of rigid crustal blocks superposed on subduction (McCaffrey et al., 2000; McCaffrey et al., 2007; McCaffrey et al., 2013; Savage et al., 2000, **Figure 4A**). One suggested driver for this inferred forearc rotation is the NNW-migration of the SNGV block, which currently moves with respect to North America at approximately 11–13 mm/yr (Argus and Gordon, 1991; Dixon et al., 2000; Plattner et al., 2010). In that scenario, the SNGV block would impose a NNW-directed force along the southern edge of the forearc causing blocks to rotate clockwise (McCaffrey et al., 2007). The motion of the SNGV is similar to the displacements produced by the MCC, so the two processes could combine to enhance the NNW-directed effects on the observed GPS velocity fields (McKenzie and Furlong, 2021). Since the SNGV block and the MTJ are moving northward at 11–13 mm/yr and 50 mm/yr respectively, their combined effect on the velocity field of southern Cascadia would have been significantly different in the past. In our analyses we use the results of McKenzie and Furlong (2021), in which they use plate reconstructions to incorporate the migrating effects of the tectonic processes that act in southern Cascadia. We show the 9 Ma, 5 Ma, and present-day kinematics of the study region using these plate reconstructions and estimate the GPS equivalent velocity field pattern (termed here synthetic paleo-GPS) over these times intervals in light of the past plate motions and the locations of the MTJ and SNGV block (**Figure 4**). We then decompose the present-day GPS velocity field into a subduction coupling and a NNW-directed component to investigate how strain related to subduction coupling, the MCC and the SNGV block motion is distributed across the southern Cascadia upper-plate. The decomposed present-day velocity fields for the full extent of the Cascadia subduction zone are shown in **Supplementary Figure S1**, and the decomposed data are in **Supplementary Table S1**. These results place constraints on where shortening strains are highest, where we would expect high uplift rates, and where shear zones are developing at present in southern Cascadia.

## Kinematic Reconstruction

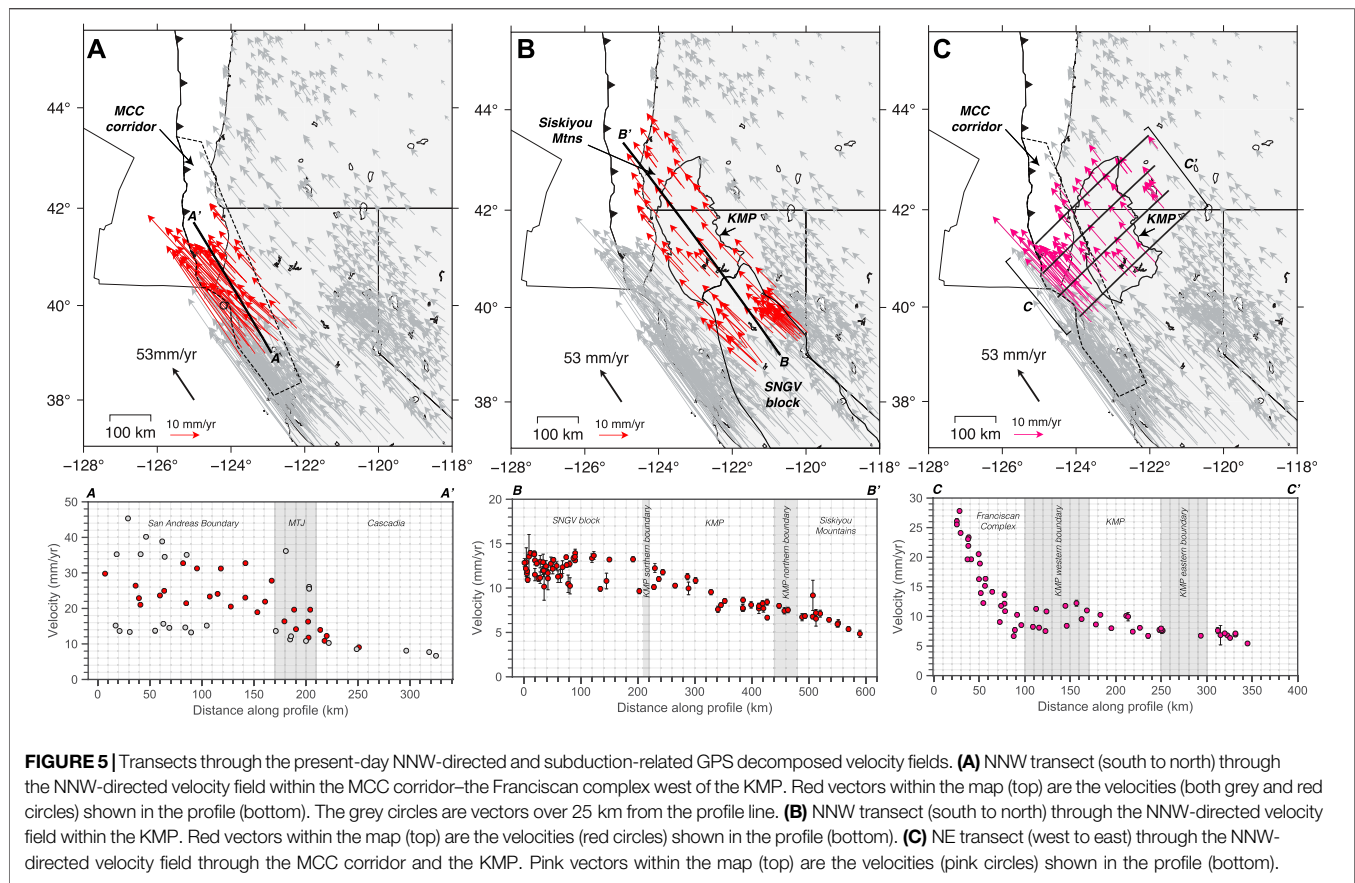
The plate kinematics for the study region at ~9 Ma, ~5 Ma and the present are shown in **Figure 4**. The synthetic paleo-GPS in **Figures 4A,B** indicate that the MCC and the motion of the SNGV

block only started to affect the upper-plate kinematics of the present-day region of southern Cascadia at ~5 Ma (**Figure 4**). The ~9 Ma reconstruction (**Figure 4A**) shows that the region of present-day southern Cascadia at ~9 Ma would be centrally located along the Cascadia margin and would have primarily been deforming as a consequence of subduction coupling processes. At this time the MTJ was significantly further south than it is today and so the effects of the MCC processes would not have reached this region. Additionally, at ~9 Ma the SNGV block was ~100 km south of its current location and had not yet started moving northward in response to motion across the northern ECSZ (Plattner et al., 2010). Also, southern Cascadia at ~9 Ma (38°N - 40°N, i.e., the region now south of the present-day MTJ) would be deforming in response to subduction coupling and the shortening effects of the MCC, but unlike today the SNGV would not have been a key driver of upper-plate deformation in the region. The apparent clockwise rotation seen today in south-central Cascadia would be muted, with the NNW-directed velocity field decaying rapidly inland. In addition, at this time (~9 Ma), there would have been a significant space between the northern end of the present-day surface expression of the SNGV block and the southern margin of the KMP. The two terranes are currently adjacent, suggesting the material in this gap has either shortened and led to crustal thickening or underthrust the KMP. Seismicity and several east and northeast-oriented faults and folds in the northernmost region of the Great Valley and surrounding regions are indicative of north-south/northwest-southeast shortening between the Great Valley block and KMP (Unruh et al., 2003; Unruh and Humphrey, 2017; Angster et al., 2020), suggesting that at least some of this gap-closure is accommodated by upper-plate shortening.

From ~5 Ma, the present-day region of southern Cascadia may have started to display the apparent rotation that we see in the GPS velocities today (**Figure 4B**), in response to the MTJ northward migration and the onset of SNGV-related deformation. **Figure 4** highlights that over the past ~10 million years, the key drivers of deformation in present-day southern Cascadia and south of the MTJ have changed, and it is only recently (since ~5 Ma) that the present-day southern Cascadia upper plate, including the KMP, has been deforming in a composite tectonic regime with subduction, MCC and SNGV deformational drivers.

## Present-Day Tectonic Components of the Cascadia GPS Velocity Field

We separate the present-day GPS velocity field into two components, a NE-oriented subduction-coupling driven component and a NNW-oriented component reflecting displacements associated with the northward motion of the MTJ and SNGV block (McKenzie and Furlong, 2021). From these two displacement components we find that both the NE-directed and NNW-directed shortening strain rates are highest within the Franciscan complex, to the west of the KMP. The KMP itself is accommodating very low NE- and NNW-oriented shortening rates of  $\sim 10^{-16} \text{ s}^{-1}$  (McKenzie and Furlong, 2021; McKenzie et al., 2022).



### NNW-Directed Deformation

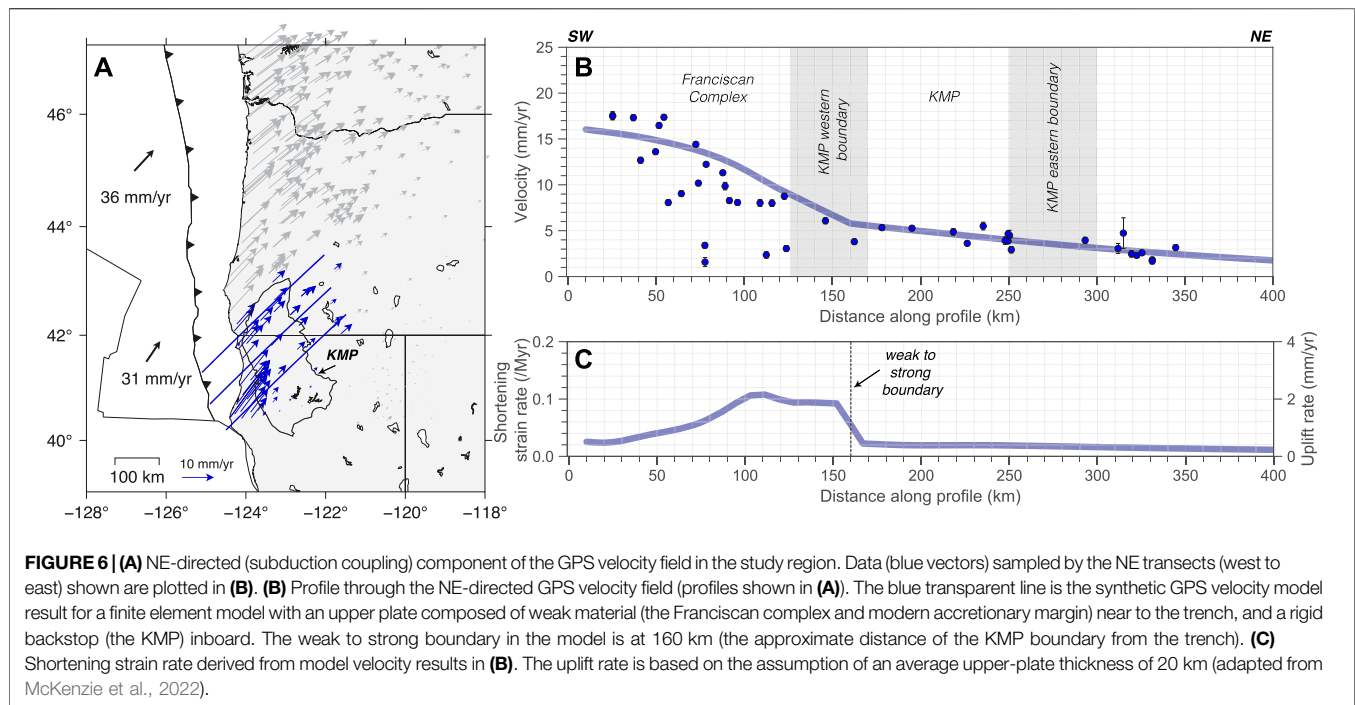
The NNW-directed GPS velocity field shows a steep decreasing gradient in velocities over a distance of  $\sim 40\text{--}50$  km (shortening strain rate of  $\sim 10^{-14} \text{ s}^{-1}$ ) north of the MTJ within a relatively narrow channel between the subduction trench to the west and the KMP to the east (**Figure 5A**). This has been interpreted to reflect crustal shortening associated with the MCC process (McKenzie and Furlong, 2021; Furlong and Govers, 1999). In contrast, to the east of the MCC corridor, the NNW-directed velocity field has a shallow decay from  $\sim 12$  mm/yr to  $8$  mm/yr from south to north across the KMP (shortening rate of  $\sim 10^{-16} \text{ s}^{-1}$ ). Although the KMP is internally experiencing low shortening rates, the northwestern-most region of the KMP [north of the Cave Junction fault, a structure inferred to mark the mountain front near Cave Junction, Oregon (Kirby et al., 2020; Kirby et al., 2021; Von Dassow and Kirby, 2017)] is currently undergoing crustal shortening at strain rates of  $\sim 10^{-15} \text{ s}^{-1}$  (**Figure 5B**). This NW region of the KMP, a portion of the Siskiyou Mountains, exhibits relatively high topographic relief compared to its surroundings, and the association of high relief, steep channels and elevated erosion rates (e.g., Balco et al., 2013) suggest that this relief may be relatively young (McKenzie and Furlong, 2021; Kirby et al., 2020, 2021). We infer that the northward velocity gradient represents the relatively rigid motion of the KMP in response to the northward motion of the SNGV-block to its south—pushing on the southern margin of the KMP and, in

turn, causing the KMP to impinge on the region of the Siskiyou Mountains (McKenzie and Furlong, 2021). This push on the southern margin of the KMP, leads the KMP to move relatively rigidly to the NNW with respect to North America.

In addition to NNW-directed shortening, we observe right-lateral differential motion between the Franciscan crust within the MCC corridor and the KMP (**Figure 5C**). This differential motion implies a narrow zone of NNW-oriented right lateral shear adjacent to the KMP's western boundary. This localized region of right-lateral shear spatially coincides with a zone of upper-plate forearc translational faults inboard of a zone of forearc compression (Kelsey and Carver, 1988). The zone of forearc translation contains several NNW-oriented faults including the Grogan fault, the Lost Man fault and the Bald Mountain fault zone to the north, and the Eaton Roughs and Lake Mountain fault zones further south (Kelsey and Carver, 1988; **Figure 1**). These faults are optimally oriented for NNW-oriented right-lateral shear produced by MCC- and SNGV-driven components.

### Subduction Earthquake Cycle Deformation

The NE-component of the GPS velocity field reflects how the upper plate is being deformed in response to subduction plate interface coupling along the Cascadia margin. Similar to the



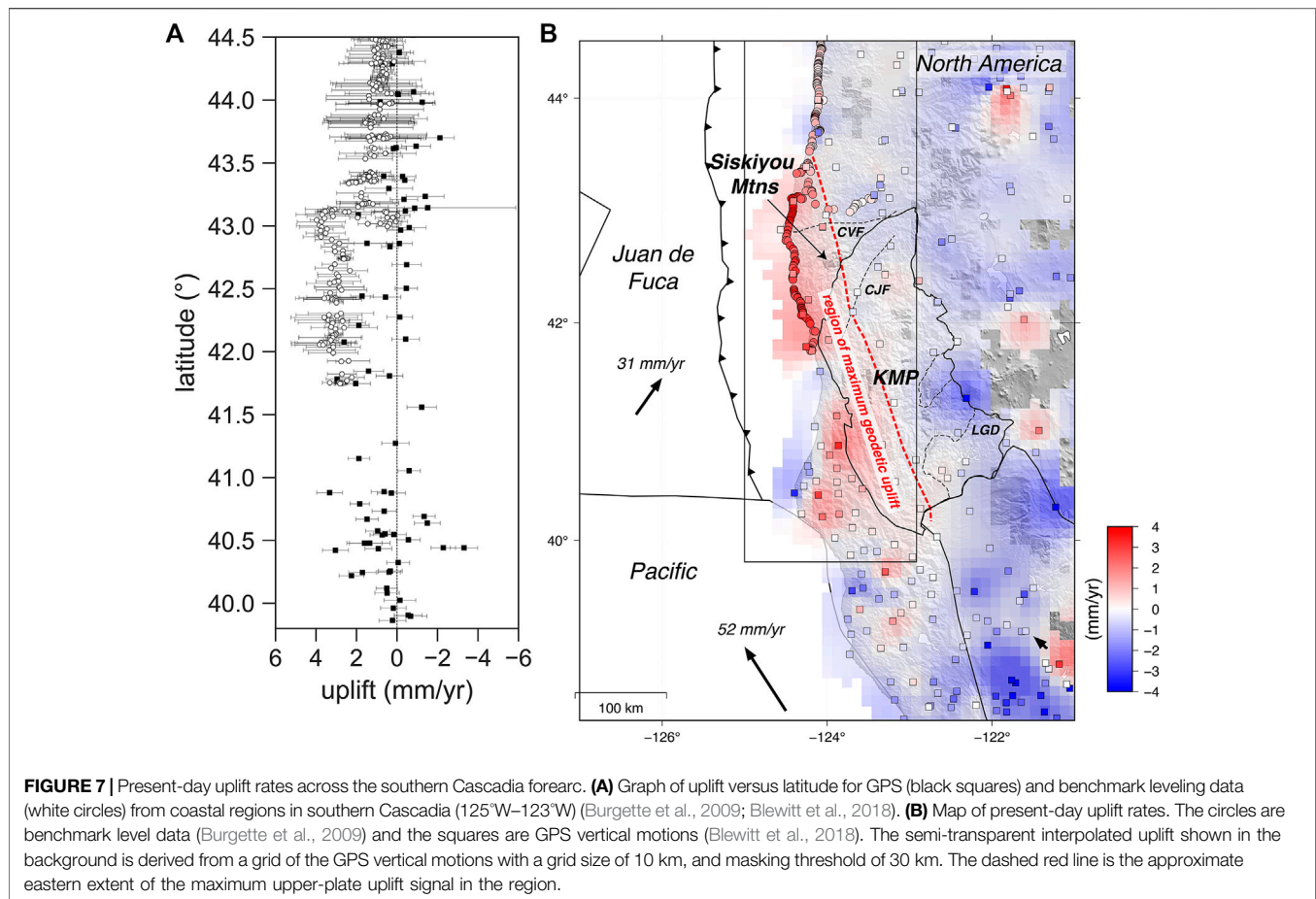
NNW-component, the subduction component of the GPS velocity field shows a localized region of shortening within the Franciscan complex, west of the KMP. This is characterized by a steep gradient in the NE-directed surface velocities from  $\sim 17$  mm/yr to  $\sim 5$  mm/yr over a distance of  $\sim 125$  km within the Franciscan complex—a shortening strain rate of  $\sim 10^{-15} \text{ s}^{-1}$  (Figure 6). East of the Franciscan complex within the KMP, the NE-directed GPS velocities remain at  $\sim 5$  mm/yr across the region (Figure 6). This localization of shortening within the weak Franciscan material can be linked to the effects of subduction mechanical locking terminating within the relatively weak crustal domain (the Franciscan complex) to the west of a rigid backstop - the KMP (McKenzie et al., 2022). In regions where subduction locking ends trenchward of a rigid backstop, interseismic subduction-related shortening is localized in the region between the down-dip limit of locking and the rigid backstop (McKenzie et al., 2022). The upper-plate region in southern Cascadia that is experiencing localized subduction-related shortening due to this effect is also within the northern part of the MCC-corridor. Further north, the weak-to-strong boundary is significantly closer to the trench (the Franciscan complex is absent, and Siletz-Crescent terrane extends offshore) and locking extends beneath this weak-to-strong transition. McKenzie et al. (2022) find that in that case there is only a narrow region of localized shortening offshore, west of the Siletz-Crescent terrane. Additionally the relatively strong Siletz-Crescent terrane extends the subduction coupling signal far inland since it does not shorten easily.

The subduction-related displacements observed by the geodetic stations are largely elastic and recovered during large

megathrust events. However, typical of subduction zones globally, some fraction of this elastic deformation is retained as permanent upper-plate deformation over multiple subduction earthquake cycles (e.g., Melnick et al., 2006; Meltzner et al., 2006; Saillard et al., 2017; Ramírez-Herrera et al., 2018; McKenzie et al., 2022). In contrast, the MCC-process produces permanent crustal shortening over millions of years, adjacent to and in advance of the MTJ. Although the geodetic signal can be separated into subduction and NNW-components and records both elastic (subduction) and permanent (subduction and MCC) deformation, the long-term deformation recorded—for example by slip on upper-plate faults and permanent uplift of the coastline—records the combined effects of permanent subduction and MCC deformation, which are not easily separated.

## Vertical Motions

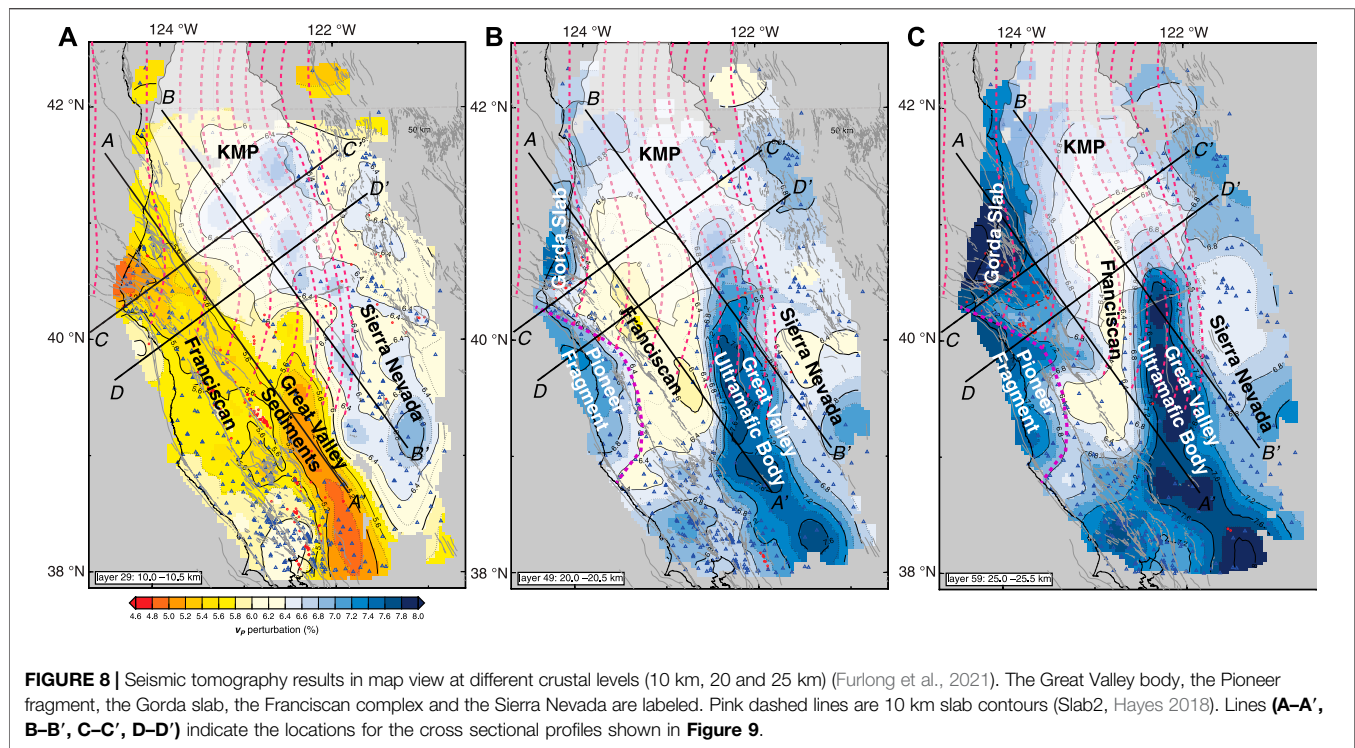
Unlike the horizontal components of the GPS velocity field, the vertical component cannot be decomposed into separate signals related to different tectonic drivers based on direction. Instead the geodetic uplift/subsidence signal records the combined vertical motions produced by all tectonic drivers in the region. Thus, although we observe present-day vertical motions of 1–4 mm/yr, by GPS and other geodetic indicators in the MCC corridor (Burgette et al., 2009; Blewitt et al., 2018) (Figure 7), we cannot separate this into a subduction-coupling and MCC signal without prior subduction locking or MCC-model assumptions.



The subduction component of the vertical motion during the inter-earthquake interval largely depends on the location of the site relative to locking on the subduction plate interface and the time since the last megathrust earthquake. If the site lies above a locked region, we expect to record subsidence, however when the site is inboard of the locked region it could record subsidence, uplift or zero present-day vertical motion depending on the details of the coupling (Govers et al., 2018). Some locking models for Cascadia (e.g., Schmalzle et al., 2014; Li et al., 2018; McKenzie and Furlong, 2021) find that locking extends near to and in some cases beneath the present-day coastline of Cascadia. With that configuration we would generally expect subsidence along the coastline during the interseismic period. In southern Cascadia however, crustal thickening associated with the MCC-process produces some uplift in the vicinity of the MCC spatial footprint (Figure 4; Furlong and Govers, 1999). As a result, where the MCC process and subduction are both contributing to the vertical motions (within the MCC corridor), the observed total GPS velocity field records the summation of both processes. In cases where the subduction coupling signal is subsidence, the addition of MCC uplift may reduce that subsidence or even combine to produce uplift. In regions where the subduction coupling signal is uplift, the MCC contribution would increase the observed uplift.

## SEISMIC TOMOGRAPHY CRUSTAL STRUCTURE

The MCC model involves upper-plate crustal shortening and thickening in advance of the migrating MTJ, and subsequent crustal thinning after passage of the MTJ (Furlong and Govers, 1999). How that crustal thickening is converted into upper-plate deformation is less clear since the MCC model did not place constraints on potential out-of-plane deformation or specify deformation mechanisms for the shallow crust (Furlong and Govers, 1999). Additionally, the geologic structure of the region affected by MCC deformation is varied, that is the crust involved has changed substantially over the past 9–10 million years (Figures 3, 4). Prior to ~10 Ma, the region of MCC shortening/thickening was bounded on the east by the SNGV block (Figures 2–4). However, by ~5 Ma as the MTJ migrated northward, the upper-plate geologic framework in southern Cascadia underwent a transition from a Franciscan-Great Valley to a Franciscan-KMP configuration (Figures 3, 4). This suggests that prior to 5 Ma the SNGV block was playing a similar role in upper-plate deformation to the KMP today. To understand how the MCC and SNGV affect upper-plate deformation, including permanent uplift and the development of shear zones, we use the results from a recent seismic



tomography study (Figures 8, 9; A. Villaseñor, K.P. Furlong, H. Benz, *personal communication*; Furlong et al., 2021), to identify the 3D crustal nature of the processes that are driving upper-plate deformation (specifically crustal thickening and thinning, permanent uplift, and faulting). Based on this present-day 3D crustal structure and plate reconstructions of the region (Figures 2, 4), we can explore how the crustal structure and upper-plate deformation associated with each of these tectonic processes has evolved over time.

This seismic tomography imagery (Figures 8, 9) shows systematic differences in the overall pattern of MCC crustal thickening behavior in the region bounded on the east by the SNGV block (south) versus the KMP (north). Horizontal depth slices and cross-sectional profiles highlight the primary characteristics of the crustal structure in the region. There is a significant contrast in seismic velocity properties between the meta-sedimentary Franciscan complex and the adjacent SNGV block and KMP. South of the MTJ, the Franciscan complex ( $p$ -wave velocities ( $V_p$ ) of  $\sim 5.6$ – $6.4$   $\text{km s}^{-1}$ ) and MCC crustal deformation (thickening/thinning) is bounded on the east by the SNGV block ( $V_p \sim 6.8$ – $8.0$   $\text{km s}^{-1}$ ), and on the west by the Pioneer Fragment ( $V_p \sim 6.8$ – $8.0$   $\text{km s}^{-1}$ ). North of the MTJ the Franciscan complex is bounded on the west by the Gorda slab ( $\sim 6.8$ – $8.0$   $\text{km s}^{-1}$ ). However, to the east we see that the Franciscan rocks impinge on and into the KMP crust ( $V_p \sim 6.4$ – $6.8$   $\text{km s}^{-1}$ ) (Figures 8, 9).

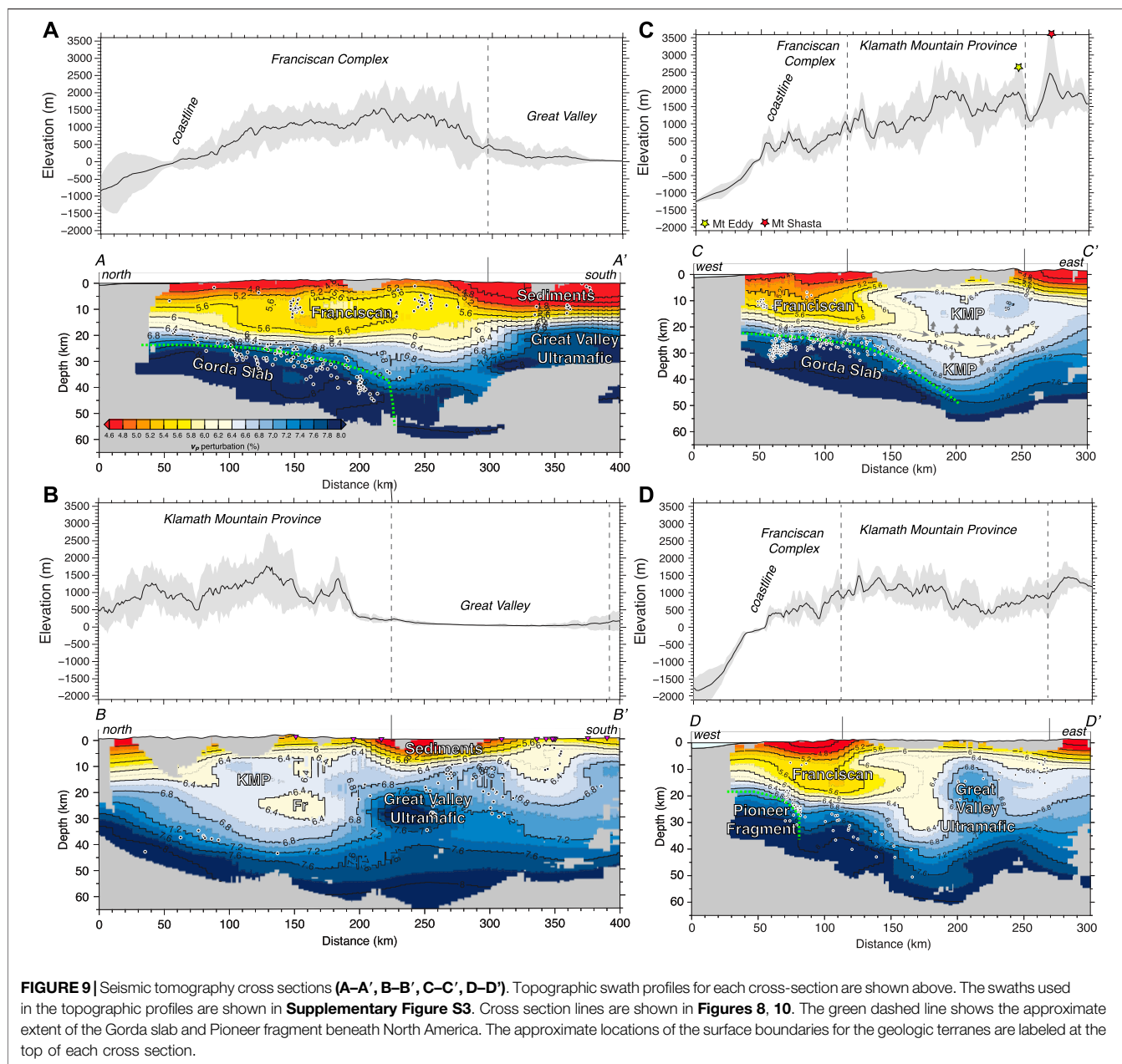
This implies that MCC driven upper-plate deformation was, and is still, localized within the Franciscan complex when adjacent to the SNGV block. In contrast, MCC-related deformation appears to extend into the KMP crust, north of the SNGV block. In particular, a region of Franciscan crust

appears to have intruded  $>30$  km into the SW region of the KMP at  $\sim 10$ – $30$  km depth (Figures 8, 9). Associated with this, there is a  $\sim 10$  km thick tubular body of what we interpret to be Franciscan material, that extends an additional  $\sim 80$  km east into the KMP at  $\sim 20$ – $30$  km depth (Figures 8, 9). This injected/intruded crustal material ( $V_p$   $6.0$ – $6.4$   $\text{km s}^{-1}$ ) has an oblate cylindrical shape and is surrounded by the higher velocity crustal material of the KMP. We take this to indicate a form of crustal flow as the Franciscan complex is over-thickened as part of the MCC process and is then able to wedge or inject itself into the adjacent KMP crust.

As well as this intrusion of the Franciscan material into the KMP crust primarily from the west-southwest, there is a separate region of high  $p$ -wave velocity ( $\sim 6.8$ – $7.6$   $\text{km s}^{-1}$ ) material lying at  $\sim 15$ – $30$  km depth beneath the south-eastern region of the KMP crust. This high velocity body can be seen to be a continuation of the Great Valley ultramafic body to the south and appears to extend  $\sim 50$ – $100$  km beneath the KMP to the north (Figures 8, 9B). In contrast to the injected Franciscan crust, this material appears to lie below the KMP crust, underthrusting the SE margin of the KMP.

## Discussion of Seismic Tomography Results

The crustal-scale plate boundary structure plays an important role in the patterns of upper-plate deformation produced by the tectonic processes acting in southern Cascadia. In particular, crustal kinematics and deformation driven by the MCC process and SNGV motion correlate well with many of the regions of ongoing deformation. We see evidence (e.g., thickened crust adjacent to the southern edge of the Gorda slab, that thins to the south) of the effects of MCC crustal



deformation in the tomography imagery (**Figures 8, 9**) associated with the transition from subduction to translation. There are several instances where the crustal structure observed in the tomography differs from that expected from the MCC model (Furlong and Govers, 1999). We interpret these to reflect differences in the way that MCC crustal thickening is accommodated in the North American upper plate.

The MCC-driven thickened crust in the region currently south of the present-day MTJ occurred when that location was the southernmost part of the Cascadia subduction plate boundary as the MTJ was approaching (Furlong and Govers, 1999). For example, at ~9–10 Ma, when the MTJ was located substantially further south (**Figures 2, 3**), the locus of MCC

shortening and crustal thickening (at and north of the MTJ) would have been bounded on the east side by an abrupt transition from the Franciscan complex to the Great Valley crust. The region of MCC-related deformation is always bounded on the west by the subducting plate (north of the MTJ) and the Pioneer Fragment (**Figures 2, 3, 8, 9**) immediately south of the MTJ—since both features migrate with the MTJ. The result of this Franciscan-bounding crustal structure is that when the MTJ was south of approximately 39°N, the corridor of MCC-deformation would have been restricted to a narrow channel of the Franciscan complex between the Pioneer Fragment and the SNGV block. This is seen in the narrow width (<100 km) of the thickened low seismic-velocity material in that region.

Over the past 3–5 million years, with the continued northward migration of the MTJ and SNGV block, the eastern margin of the MCC corridor changed from being defined by the SNGV block to the KMP. Prior to the switch to the KMP, the MCC deformational channel widened as a result of the northern segment of the Great Valley ultramafic block being oriented more northward (**Figure 2**). This switch from SNGV to the KMP acting as the eastern boundary to the deformational channel has also led to a substantial change in how MCC crustal thickening is accommodated. North of the MTJ, the MCC crustal thickening is still bounded on the west by the subducting slab but seems to intrude into (or otherwise be emplaced within) the KMP crust. This low seismic-velocity Franciscan material appears to wedge the KMP crust apart, and flow and inject itself into the existing KMP crust (**Figures 8, 9**); i.e. we see that the low-velocity material lies between two regions of KMP crust. Additionally, this low-velocity intrusion is not planar, as might be expected for a situation where the KMP over-thrusts the Franciscan crust. Instead, as seen in the tomographic cross-sections (**Figure 9**), it is a cylindrical intrusion within the KMP crust. For these reasons and its continuity to the Franciscan complex we interpret the low-velocity material to be injected Franciscan crust that has undergone crustal flow in its emplacement.

Other possible explanations for this intra-crustal low-velocity material such as lithologic variations within the KMP, or thermal variations are harder to explain based on the geometry and extent of the region of anomalous crust. Additionally, starting at ~6 Ma, the SNGV block began to accelerate (Plattner et al., 2010), converging with and pushing the KMP ahead of it. The tomography results imply that as part of that convergence, Great Valley material that was initially in the gap between the SNGV and KMP prior to SNGV movement, appears to underthrust the southeastern margin of the KMP. (**Figures 8, 9**). During the Eocene to Miocene, exhumation (Batt et al., 2010; Piotraschke et al., 2015) of material in the footwall (north) of the La Grange fault lead to crustal thinning in the hanging wall to the south. This region of La Grange crustal thinning could have provided the space where we observe the northern limit of the emplaced Great Valley body beneath the KMP crust, potentially having replaced this previously exhumed material. This region of impingement or underthrusting of the northern limits of the Great Valley body also serves as an eastern and southern bounding constraint on the region of the Franciscan crustal flow within the KMP, producing a nose-like protuberance of the lower-velocity material across the KMP.

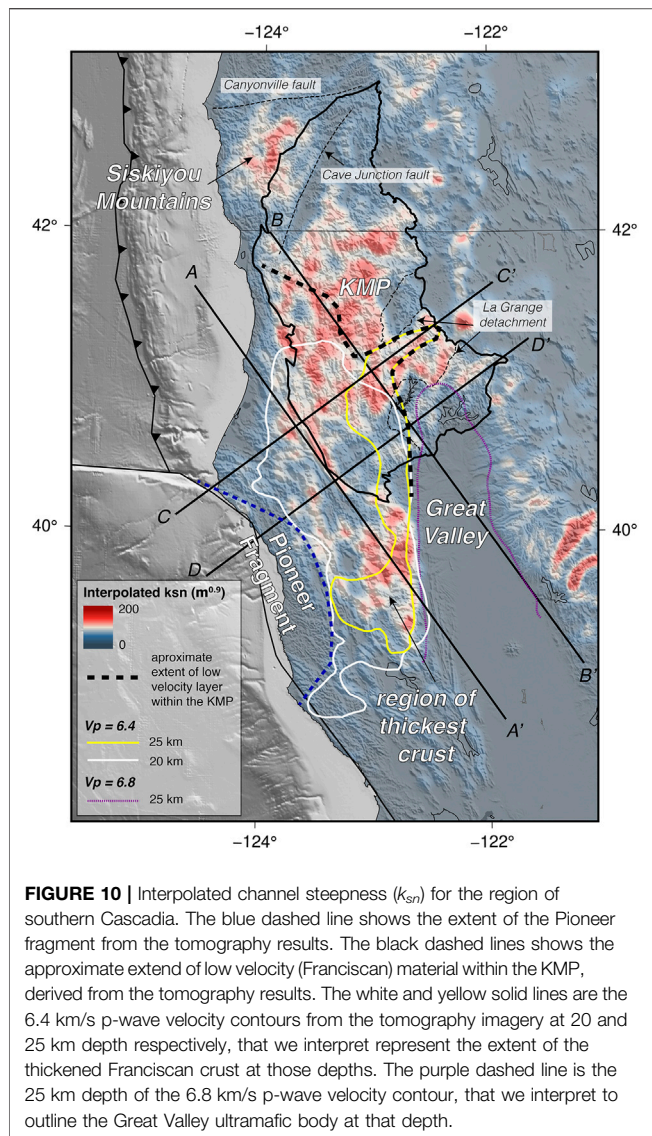
We interpret this major change in how MCC crustal deformation is accommodated, predominantly within the Franciscan complex and its interaction with the adjacent KMP, to generate different styles of upper-plate faulting and uplift throughout the region. In particular, patterns of upper-plate faulting and uplift in present-day southern Cascadia and the KMP are likely to be geologically recent (since ~5 Ma) - since most crustal shortening/thickening in the MCC model occurs at and just to the north of the MTJ. In contrast, at latitudes south of ~39°N (i.e., located in southern Cascadia at ~10–5 Ma), MCC upper-plate deformation was restricted to a narrow zone <100 km in width, bound by the rigid Great Valley block to

the east. Since 5 Ma, this corridor of Franciscan material has been able to expand laterally (>50 km) into the KMP. Thus, prior to ~5 Ma we expect topographically a relatively narrow “ridge” (<100 km wide) of uplift in the MCC corridor and from ~5 Ma to the present, we see that the MCC-shortening zone has widened across the boundary between the Franciscan and KMP crust. Therefore, the upper-plate deformational response to the MCC in present-day southern Cascadia, including the KMP, should be relatively recent (<5 Ma), since it is only from 5 Ma that MCC deformation has been active in that region (**Figures 3, 4**).

The study area straddles the southern edge of the subducting Gorda slab and in addition to the effects that this location has on processes such as the MCC, the behavior of the southern slab edge has also been proposed to affect asthenospheric mantle flow in the region (Zandt and Humphreys, 2008). Zandt and Humphreys (2008) proposed that if there is significant rollback of the Gorda slab that mantle flow could be induced around the southern edge of the slab, akin to the mantle flow inferred around the northern edge of the subducting Pacific slab at Tonga (e.g., Foley and Long, 2011). As discussed by Zandt and Humphreys (2008), such mantle flow is a longer wavelength feature that would be centered to the east, within (and underlying) the Basin and Range province. It also would likely be at greater depths than we are considering in this work, thus would have only a minor impact on our study region. Results of previous studies of mantle anisotropy along coastal North America indicate that our study region is within the mantle flow realm primarily affected by the local subduction and the lithospheric slab window. As shown by Hartog and Schwartz (2000) the upper-most mantle anisotropy within the subduction domain is consistent with down-dip to the east flow, and in the slab window south of the southern edge of the Gorda slab, the mantle flow is similarly dipping down to the east likely indicating mantle upwelling into the slab window from the adjacent mantle wedge, consistent with the geochemistry of the Coast Range volcanics erupted above the slab window (Furlong et al., 2003). The crustal flow of the Franciscan crust that we interpret to occur in the middle and lower crust, is separated from the upper-mantle flow regime by the lower crust and lithospheric mantle of the North American plate.

## Is the Klamath Mountain Province Undergoing Active Uplift?

The crustal structure, as seen in the tomography results, strongly correlates with the present day topography in the Klamath and Siskiyou Mountains (**Figure 9**). We can see in the various tomographic profiles a correlation between subsurface crustal structure (in particular, thickness of the Franciscan complex) and elevation. For example in profile A-A' (**Figure 9A**) the systematic thickening of the Franciscan crust (from ~20 km to ~30–35 km) in association with MCC crustal deformation correlates with a nearly 2 km elevation change along the profile. The abrupt decrease in crustal thickness and change in composition as the profile crosses from the Franciscan Coast Ranges to the Great Valley is seen in a substantial drop in elevation.



Perhaps more diagnostic of the link between crustal structure and elevation are the correlations seen in profiles B-B' and C-C' (Figures 9B,C). These profiles cut across the intruded nose of the Franciscan complex that we interpret to be intruded or injected into the KMP crust. The maximum elevation occurs at ~120–150 km along profile B-B', crossing this region. Profile C-C', which runs along the length of this Franciscan “nose” shows a systematic increase in elevation, that culminates in the region of Mt Eddy which sits above the eastern terminus of the low velocity body. Mt Eddy is the highest elevation in the KMP, and is in a region of high local relief. We interpret that this reflects the role that this crustal injection has played in driving uplift. The coincidence of the highest elevation above the eastern end of the material may indicate the time progression of uplift as the crustal material flows eastward.

Thermochronology studies from the KMP (apatite fission track (AFT) and apatite (U-Th)/He (Batt et al., 2010; Piotraschke et al., 2015)) show that there have been two

periods of regional cooling and exhumation within the province: 1) A late Cretaceous-Paleocene episode of regional cooling and exhumation; and 2) a Middle Tertiary (Eocene-Miocene, ~45–15 Ma) more localized episode of rapid exhumation of the footwall of the La Grange detachment fault (Cashman and Elder, 2002). This faulting occurred with high slip rates of 2 mm/yr over ~30 million years (Piotraschke et al., 2015). The currently exposed surface is thought to have been brought to depths of ~2–3 km at the end of the latter unroofing event. If this exhumation event had continued to the present at moderate-high uplift rates, we would expect younger thermochronology ages as a consequence of deeper regions of the crust being exhumed. The preservation of Eocene to early Miocene Apatite (U-Th)/He ages in samples implies minimal exhumation since the main unroofing event. As a result, evidence of current exhumation likely reflects a relatively recent active process.

Despite evidence for the most recent cooling/uplift being during the Eocene to Miocene, and minimal evidence of horizontal crustal shortening, the KMP is a topographically anomalous region of the southern Cascadia forearc, exhibiting higher elevations and topographic relief than the surrounding regions (Figures 1, 10). One means of assessing whether differences in topography may be related to differential rock uplift involves looking at patterns of normalized channel steepness ( $k_{sn}$ ) across the region (e.g., Whipple and Tucker, 1999; Kirby and Whipple, 2001; Wobus et al., 2006; Kirby and Whipple, 2012). We use TopoToolbox 2 (Schwanghart and Scherler, 2014) to calculate the normalized channel steepness across the region using a reference concavity of 0.45 and create a smoothed  $k_{sn}$  map shown in Figure 9. The drainage network  $k_{sn}$  map used in the interpolation is shown in Supplementary Figure S2. When we compare these results to the seismic tomography imagery, we find there are spatial correlations between  $k_{sn}$  at the surface and inferred tectonic processes at depth.

Our results show three key regions of elevated  $k_{sn}$ :

- 1) There is a region of high  $k_{sn}$  in the northwestern-most KMP and the Siskiyou Mountains (Figure 10). This region is coincident with the highest present-day geodetic and benchmark (tide gauge and leveling) uplift rates observed along the Cascadia coastline (Figure 7, Blewitt et al., 2018; Burgette et al., 2009), and preliminary assessment of erosion and fluvial incision rates (Balco et al., 2013; Von Dassow and Kirby, 2017) suggest that this region is experiencing elevated erosion rates relative to the forearc to the north and west (Kirby et al., 2020).
- 2) A large portion of the KMP itself has high values of  $k_{sn}$  compared to its surroundings, specifically between 41°N and 42.5°N. This area overlaps with the northern region of the low velocity intracrustal region imaged in the tomography, that we interpret to be an intrusion of Franciscan material into the KMP (Figure 10). This area is also in the footwall of the La Grange detachment fault, that underwent a period of exhumation during the Eocene to Miocene (Batt et al., 2010; Piotraschke et al., 2015).

- 3) South of the KMP there is a region of high  $k_{sn}$  in the Yolla Bolly mountains that coincides with the thickest region of the MCC-thickened crust (Figures 8, 10).

These observations suggest that there are three regions of the southern Cascadia forearc that may currently be experiencing (or have very recently experienced) active tectonic uplift. In particular, the interior of the KMP may be undergoing a recent rejuvenation in uplift, perhaps associated with the onset of MCC- and SNGV-related deformation at ~6–5 Ma.

## Possible Causes of Recent Uplift Across Southern Cascadia

### Uplift Within the Northwest Klamath Mountain Province and Siskiyou Mountains

The region of the northwestern-most KMP and the Siskiyou Mountains has both high  $k_{sn}$  and is experiencing some of the highest rates of present-day (2–4 mm/yr) uplift across the Cascadia margin (Blewitt et al., 2018; Burgette et al., 2009, Figure 7). Uplifted marine terraces along the coast at these latitudes also indicate high long-term uplift rates (~0.25–0.9 mm/yr, Kelsey and Bockheim, 1994; Kelsey et al., 1994). Present-day horizontal GPS motions show significant NE- and NNW-directed shortening strain in the region (Figures 5, 6). McKenzie and Furlong (2021) proposed that this NNW-directed shortening strain may be driven by the push of the SNGV block along the KMP's southern boundary. In addition to this NNW-directed tectonic driver, the results of McKenzie et al. (2022) imply that this region of the Cascadia upper plate, between the down-dip limit of coupling and an upper-plate rigid backstop will be undergoing high rates of localized subduction-related shortening in response to coupling on the plate interface. The combination of subduction-related shortening strain and NNW-directed shortening strain could explain the high present-day geodetic uplift and high topographic relief in this region.

### Rejuvenation of Uplift of the Klamath Mountain Province

The subduction and NNW-directed components of the GPS velocity field show that at present the KMP is accommodating low rates of NE- and NNW-oriented shortening ( $\sim 10^{-16} \text{ s}^{-1}$ ) (Figures 5, 6). Thus, bulk crustal thickening of the KMP is an unlikely mechanism for driving recent uplift. We have interpreted the intracrustal low velocity body in the seismic tomography slices (Figures 8, 9) to be Franciscan crustal material that has thickened and intruded into the KMP at mid-crustal levels as a consequence of crustal flow. We hypothesize that localized NNW-directed shortening, superimposed on NE-directed subduction-driven deformation, enables Franciscan crust to intrude into the KMP along a plane of weakness at depth. This injection of additional crustal material at depth into the KMP, would drive differential rock uplift within the KMP, providing an explanation for relatively recent uplift and

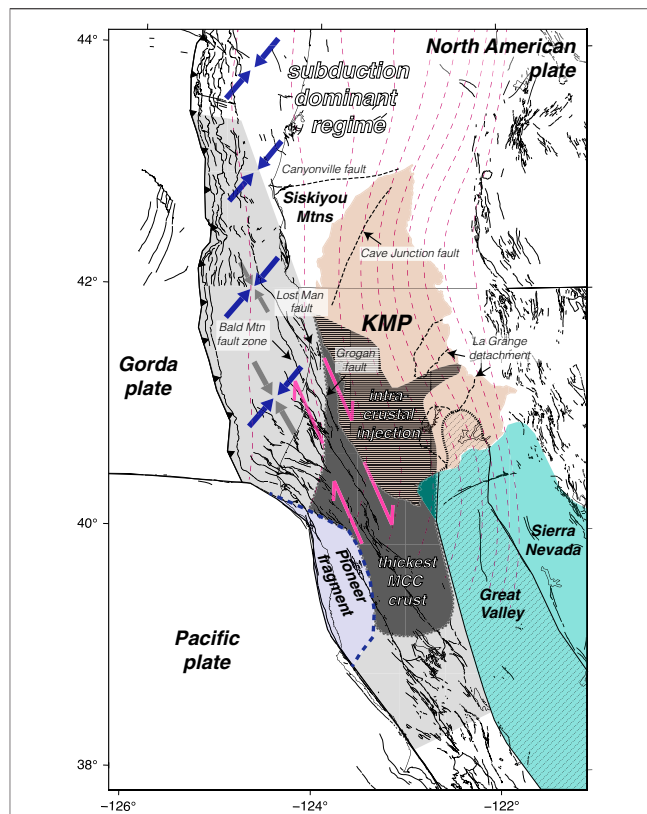


**FIGURE 11 |** Summary map showing the tectonic setting, geographic regions, and key tectonic processes acting in the study region that produce upper-plate deformation of the North America plate. North of ~43°N subduction-coupling is the dominant tectonic process acting to deform the upper plate. The light grey shaded region shows the approximate N-S extent of the MCC process on the upper plate. The dark grey shading shows the region of the highest crustal thickness within the MCC corridor, outlined based on the 20 km depth tomography imagery. The horizontal dashed region within the KMP, shows the approximate extend of the Franciscan crustal material injected into the KMP at mid-crustal levels. The Pioneer fragment is shaded in light blue. The teal shaded region is the SNGV block. The dotted lined region within the SNGV block shows the approximate extent of the Great Valley ultramafic body at mid-crustal levels.

generation of topographic relief. These effects associated with the MCC have only been affecting upper-plate deformation in this region since ~5 Ma (Figure 4).

### Uplift Within the Southern Mendocino Crustal Conveyor Corridor

South of the KMP, the region of high  $k_{sn}$  correlates with the thickest (>30 km thick) crust within the MCC corridor (Figures 8–10). South of this region the extensional (later stage) effects of the MCC are expected, and we see a systematically thinning crust, and active volcanism within the Clear Lake Volcanic field (Furlong and Govers, 1999; Furlong and Schwartz, 2004). This region of the upper plate is where the MCC model shows a transition from shortening strain (to the north) to extensional strain (to the south), and thus we might expect that this region—in response to MCC effects—should not be experiencing significant active uplift at present (Furlong and Govers, 1999). However, a

few million years ago this region would have been shortening and thickening, similar to the upper plate currently in the vicinity of the MTJ. Thus, this region of high  $k_{sn}$  may be recording the channel response to a transition from an actively shortening to an actively thinning crust.

## FAULTING AND SHEAR ZONE DEVELOPMENT

In addition to numerous accretionary margin faults linked to displacements on the megathrust detachment offshore near to the trench, there are several active crustal-scale upper-plate structures onshore within the Franciscan and KMP crust. In southern Cascadia, these faults are being loaded by the composite set of forces associated with both subduction and NNW-directed shortening and shear (Kelsey and Carver, 1988; McCrory, 2000; McKenzie and Furlong, 2021). Additionally, with the generally NNW/NW strike of these faults (e.g., the Grogan fault, **Figure 11**), they are optimally oriented for both reverse dip-slip in response to subduction-related SW-NE shortening and right-lateral shear motion west of the KMP (**Figures 5, 11**). As the MTJ migrates northward, these faults are well oriented to participate in the developing San Andreas plate boundary. These faults potentially undergo a change in their behavior over time from dominantly dip-slip to dominantly strike-slip motion as the MTJ approaches and the plate boundary transitions from subduction to transform. Initially, such faults would likely exhibit reverse motions, due to subduction coupling related NE-directed shortening of the upper plate. As the MTJ moves further north, a right-lateral shear zone develops along the western margin (**Figures 5, 11**). As a consequence, NNW-oriented faults within the right-lateral shear zone, such as the Grogan fault, the Lost Man fault and faults within the Bald Mountain fault zone (**Figure 11**) are loaded by both right-lateral shear strain and subduction-related shortening strain. During this time interval, these faults could experience reverse, oblique or right-lateral motion. As the MTJ continues its northward advance and this upper-plate crust transfers from the Cascadia subduction zone to the San Andreas (Pacific-North America) plate boundary, the NNW-oriented faults become loaded by right-lateral shear stresses, developing further as San Andreas plate boundary structures.

It is unclear when these subduction zone upper-plate faults are primarily active—whether coincident with megathrust rupture or during times between major subduction zone events. There is a set of faults that occupy a similar location within the transition zone at the southern end of the Hikurangi subduction zone (in northern South Island, New Zealand) to strike-slip motion along the Alpine fault system (Furlong and Herman, 2017). These upper-plate faults experienced extreme vertical and strike-slip motion during the 2016 Kaikoura megathrust earthquake (Hamling et al., 2017), which involved simultaneous rupture of the megathrust and these upper-plate faults. If the equivalent upper-plate faults in southern Cascadia behave similarly, this could explain the large, permanent vertical motion observed along the southern Cascadia coastline, documented by uplifted marine terrace platforms (Kelsey,

1990; Muhs et al., 1992; Kelsey and Bockheim, 1994; Kelsey et al., 1994; Padgett et al., 2019).

## CONCLUSION

The overall deformational effects on the upper plate of the southern Cascadia forearc from the superposition of multiple tectonic processes, including subduction coupling, the MCC process, and the northward motion of the SNGV block can be identified by consideration of the decadal-scale motions of the upper plate and the regional long-term geomorphic and geologic record. In regions where subduction coupling is not the sole contributor to upper-plate deformation, for example near plate boundary transition zones such as the MTJ region, understanding the upper-plate effects of superposed tectonic processes is important. Being able to separate these effects is crucial when using upper-plate observations to determine the characteristics of subduction zone processes such as plate interface coupling.

In addition to the primary role of subduction coupling, upper-plate deformation in Cascadia is also affected by shortening driven by the migration of the MTJ and SNGV block, acting on varying upper-plate lithologies, depending on the location of upper-plate terrane boundaries. From the mid-Miocene to the present, the nature of the interactions between these geological terranes with the tectonic drivers has changed significantly as a consequence of the migration of the MTJ. At ~15 Ma, the KMP was in central Cascadia and subduction coupling was the main tectonic driver in that region. At that time the primary role of the SNGV block was as the rigid backstop inboard of the Franciscan complex. As the MTJ migrated northward, the KMP became the backstop east of the Franciscan complex, and the SNGV became a driver of NNW-directed deformation in southern Cascadia.

The crustal architecture both within the primary MCC deformational corridor, and its bounding terranes, has a significant impact on how the crustal thickening and thinning occurs. South of the MTJ, the MCC-related deformation of the Franciscan complex was constrained to a relatively narrow region between the Pioneer fragment and the SNGV block, when the MTJ was further south. In this case the effects of the MCC on uplift would have been restricted to this narrow channel (**Figure 11**). In contrast, deformation of the Franciscan complex north of the MTJ, where the bounding terrane to the east is the KMP, is not constrained to a narrow channel. Instead, from seismic tomography imagery we see that in addition to crustal shortening and thickening within the MCC corridor, the thickened Franciscan complex is able to flow and intrude into the KMP at mid-crustal levels (**Figures 8, 9, 11**). This intruded Franciscan crust primarily deforms the western margin of the KMP, but there is also a narrow injection of this material further eastward into the KMP (**Figures 8, 9**). The MCC has only been contributing to upper-plate deformation in this region since ~5 Ma, and as a result this intracrustal flow and injection is most likely a relatively young feature, that will continue to propagate northward with the MTJ. Similarly, the underthrusting of the Great Valley ultramafic body beneath the SE margin of the KMP, which we interpret from the seismic tomography, could continue to propagate northward with the SNGV block. We find that the impingement of the Franciscan material and the Great

Valley ultramafic body on the KMP may be generating a rejuvenation of uplift of the KMP since ~5 Ma, inferred from high channel steepness within the interior of the KMP at present.

## DATA AVAILABILITY STATEMENT

The GPS data used in this study are from the University of Nevada Reno's Geodetic Laboratory (Blewitt et al., 2018) and can be accessed online: <http://geodesy.unr.edu/>.

The benchmark leveling data plotted in Figure 7 are from Table 1 in Burgette et al. (2009) and can be accessed online: <https://doi.org/10.1029/2008JB005679>

The seismic tomography imagery shown in Figures 8, 9 was produced by Antonio Villaseñor (Institut de Ciències del Mar, Department of Marine Geosciences) and shared via a personal communication.

## AUTHOR CONTRIBUTIONS

KM analysed the GPS and topographic data. KM, KF and EK interpreted the results. KM was the main contributor in writing

the manuscript and KM, KF and EK were involved in writing and editing the final manuscript. All authors read and approved the final manuscript.

## FUNDING

This work was supported by the National Science Foundation under the Awards EAR1757581 and EAR1758463.

## ACKNOWLEDGMENTS

We thank the National Science Foundation who provided support for this research. We thank the two reviewers for their comments that helped improve the manuscript.

## SUPPLEMENTARY MATERIAL

The Supplementary Material for this article can be found online at: <https://www.frontiersin.org/articles/10.3389/feart.2022.832515/full#supplementary-material>

## REFERENCES

- Angster, S., Wesnousky, S., Figueiredo, P., Owen, L. A., and Sawyer, T. (2020). Characterizing Strain between Rigid Crustal Blocks in the Southern Cascadia Forearc: Quaternary Faults and Folds of the Northern Sacramento Valley, California. *Geology* 49 (4), 387–391. doi:10.1130/G48114.1
- Argus, D. F., and Gordon, R. G. (1991). Current Sierra Nevada-North America Motion from Very Long Baseline Interferometry: Implications for the Kinematics of the Western United States. *Geol* 19, 1085–1088. doi:10.1130/0091-7613(1991)019<1085:CSNNAM>2.3.CO;2
- Atwater, T. (1970). Implications of Plate Tectonics for the Cenozoic Tectonic Evolution of Western North America. *Geol. Soc. America Bull.* 81 (12), 3513–3536. doi:10.1130/0016-7606(1970)81[3513:iopftf]2.0.co;2
- Balco, G., Finnegan, N., Gendaszek, A., Stone, J. O. H., and Thompson, N. (2013). Erosional Response to Northward-Propagating Crustal Thickening in the Coastal Ranges of the U.S. Pacific Northwest. *Am. J. Sci.* 313 (8), 790–806. doi:10.2475/11.2013.01
- Batt, G. E., Cashman, S. M., Garver, J. I., and Bigelow, J. J. (2010). Thermotectonic Evidence for Two-Stage Extension on the Trinity Detachment Surface, Eastern Klamath Mountains, California. *Am. J. Sci.* 310, 261–281. doi:10.2475/04.2010.02
- Beaudoin, B. C., Godfrey, N. J., Klempner, S. L., Lendl, C., Trehu, A. M., Henstock, T. J., et al. (1996). Transition from Slab to Slabless: Results from the 1993 Mendocino Triple Junction Seismic Experiment. *Geol* 24 (3), 195–199. doi:10.1130/0091-7613(1996)024<0195:TFSTR>2.3.CO;2
- Beaudoin, B. C., Hole, J. A., Klempner, S. L., and Trehu, A. M. (1998). Location of the Southern Edge of the Gorda Slab and Evidence for an Adjacent Asthenospheric Window: Results from Seismic Profiling and Gravity. *J. Geophys. Res.* 103 (B12), 30101–30115. doi:10.1029/98JB02231
- Bennett, G. L., Miller, S. R., Roering, J. J., and Schmidt, D. A. (2016). Landslides, Threshold Slopes, and the Survival of Relict Terrain in the Wake of the Mendocino Triple Junction. *Geology* 44 (5), 363–366. doi:10.1130/G37530.1
- Bennett, R. A., Davis, J. L., and Wernicke, B. P. (1999). Present-day Pattern of Cordilleran Deformation in the Western United States. *Geol* 27 (4), 371–374. doi:10.1130/0091-7613(1999)027<0371:PDPOCD>2.3.CO;2
- Bennett, R. A., Wernicke, B. P., Niemi, N. A., Friedrich, A. M., and Davis, J. L. (2003). Contemporary Strain Rates in the Northern Basin and Range Province from GPS Data. *Tectonics* 22 (2), a–n. doi:10.1029/2001TC001355
- Blewitt, G., Hammond, W., and Kreemer, C. (2018). Harnessing the GPS Data Explosion for Interdisciplinary Science. *Eos* 99. doi:10.1029/2018EO104623
- Burgette, R. J., Weldon, R. J., II, and Schmidt, D. A. (2009). Interseismic Uplift Rates for Western Oregon and Along-Strike Variation in Locking on the Cascadia Subduction Zone. *J. Geophys. Res.* 114. doi:10.1029/2008JB005679
- Cashman, S. M., and Elder, D. R. (2002). Post-nevadan Detachment Faulting in the Klamath Mountains, California. *GSA Bull.* 114 (12), 1520–1534. doi:10.1130/0016-7606(2002)114<1520:PNDFIT>2.0.CO;2
- d'Alessio, M. A., Johanson, I. A., Bürgmann, R., Schmidt, D. A., and Murray, M. H. (2005). Slicing up the San Francisco Bay Area: Block Kinematics and Fault Slip Rates from GPS-Derived Surface Velocities. *J. Geophys. Res.* 110 (B6), 3496. doi:10.1029/2004JB003496
- DeMets, C., Gordon, R. G., and Argus, D. F. (2010). Geologically Current Plate Motions. *Geophys. J. Int.* 181 (1), 1–80. doi:10.1111/j.1365-246X.2009.04491.x
- DeMets, C., and Merkouriev, S. (2016). High-resolution Reconstructions of Pacific-North America Plate Motion: 20 Ma to Present. *Geophys. J. Int.* 207 (2), 741–773. doi:10.1093/gji/ggw305
- Dickinson, W. R., and Snyder, W. S. (1979). Geometry of Triple Junctions Related to San Andreas Transform. *J. Geophys. Res.* 84 (B2), 561–572. doi:10.1029/JB084iB02p00561
- Dixon, T. H., Miller, M., Farina, F., Wang, H., and Johnson, D. (2000). Present-day Motion of the Sierra Nevada Block and Some Tectonic Implications for the Basin and Range Province, North American Cordillera. *Tectonics* 19 (1), 1–24. doi:10.1029/1998TC001088
- Ernst, W. G. (2013). Earliest Cretaceous Pacificward Offset of the Klamath Mountains Salient, NW California-SW Oregon. *Lithosphere* 5 (1), 151–159. doi:10.1130/L247.1
- Foley, B. J., and Long, M. D. (2011). Upper and Mid-mantle Anisotropy beneath the Tonga Slab. *Geophys. Res. Lett.* 38, a–n. doi:10.1029/2010GL046021
- Furlong, K., McKenzie, K. A., McKenzie, K., Villaseñor, A., and Benz, H. (2021). Linkage between Upper-Plate Cascadia Faulting and the Evolution of the Northern San Andreas Plate Boundary Fault System. *GSA Connects* 2021, Portland, Oregon: Paper No. 36-2. *Geol. Soc. America Abstr. Programs* 53, 6. doi:10.1130/abs/2021AM-367654

- Furlong, K. P., and Govers, R. (1999). Ephemeral Crustal Thickening at a Triple junction: The Mendocino Crustal Conveyor. *Geol* 27 (2), 127–130. doi:10.1130/0091-7613(1999)027<0127:ECTAAT>2.3.CO;2
- Furlong, K. P., and Herman, M. (2017). Reconciling the Deformational Dichotomy of the 2016 M W 7.8 Kaikoura New Zealand Earthquake. *Geophys. Res. Lett.* 44 (13), 6788–6791. doi:10.1002/2017GL074365
- Furlong, K. P. (1984). Lithospheric Behavior with Triple Junction Migration: an Example Based on the Mendocino Triple junction. *Phys. Earth Planet. Interiors* 36 (3–4), 213–223. doi:10.1016/0031-9201(84)90047-5
- Furlong, K. P., Lock, J., Guzowski, C., Whitlock, J., and Benz, H. (2003). The Mendocino Crustal Conveyor: Making and Breaking the California Crust. *Int. Geology. Rev.* 45 (9), 767–779. doi:10.2747/0020-6814.45.9.767
- Furlong, K. P., and Schwartz, S. Y. (2004). Influence of the Mendocino Triple Junction on the Tectonics of Coastal California. *Annu. Rev. Earth Planet. Sci.* 32, 403–433. doi:10.1146/annurev.earth.32.101802.120252
- Godfrey, N. J., Beaudoin, B. C., and Klempner, S. L.; Mendocino Working Group (1997). Ophiolitic Basement to the Great Valley Forearc basin, California, from Seismic and Gravity Data: Implications for Crustal Growth at the North American continental Margin. *GSA Bull.* 109 (12), 1536–1562. doi:10.1130/0016-7606(1997)109<1536:OBTTGV>2.3.CO;2
- Govers, R., Furlong, K. P., van de Wiel, L., Herman, M. W., and Broerse, T. (2018). The Geodetic Signature of the Earthquake Cycle at Subduction Zones: Model Constraints on the Deep Processes. *Rev. Geophys.* 56 (1), 6–49. doi:10.1002/2017RG000586
- Guzowski, C. A., and Furlong, K. P. (2002). Migration of the Mendocino Triple junction and Ephemeral Crustal Deformation: Implications for California Coast Range Heat Flow. *Geophys. Res. Lett.* 29 (1), 1212–1214. doi:10.1029/2001GL013614
- Hamling, I. J., Hreinsdóttir, S., Clark, K., Elliott, J., Liang, C., Fielding, E., et al. (2017). Complex Multifault Rupture during the 2016 M W 7.8 Kaikōura Earthquake, New Zealand. *Science* 356 (6334), 356. doi:10.1126/science.aam7194
- Hartog, R., and Schwartz, S. Y. (2000). Subduction-induced Strain in the Upper Mantle East of the Mendocino Triple Junction, California. *JGR: Solid Earth* 105 (B4), 7909–7930. doi:10.1029/1999JB900422
- Hayes, G. (2018). Slab2 - A Comprehensive Subduction Zone Geometry Model. *U.S. Geol. Surv. Data release.* doi:10.5066/F7PV6JNV
- Irwin, W. P. (1985). “Age and Tectonics of Plutonic Belts in Accreted Terranes of the Klamath Mountains, California and Oregon,” in *Tectonostratigraphic Terranes of the Circum-Pacific Region: Circum-Pacific Council for Energy and Mineral Resources, Earth Science Series Number 1*. Editor D. G. Howell, 187–199.
- Kelsey, H. M., and Bockheim, J. G. (1994). Coastal Landscape Evolution as a Function of Eustasy and Surface Uplift Rate, Cascadia Margin, Southern Oregon. *GSA Bull.* 106, 840–854. doi:10.1130/0016-7606(1994)106<0840:CLEAAF>2.3.CO;2
- Kelsey, H. M., and Carver, G. A. (1988). Late Neogene and Quaternary Tectonics Associated with Northward Growth of the San Andreas Transform Fault, Northern California. *J. Geophys. Res.* 93 (B5), 4797–4819. doi:10.1029/JB093iB05p04797
- Kelsey, H. M., Engebretson, D. C., Mitchell, C. E., and Ticknor, R. L. (1994). Topographic Form of the Coast Ranges of the Cascadia Margin in Relation to Coastal Uplift Rates and Plate Subduction. *J. Geophys. Res.* 99 (B6), 12245–12255. doi:10.1029/93JB03236
- Kelsey, H. M. (1990). Late Quaternary Deformation of Marine Terraces on the Cascadia Subduction Zone Near Cape Blanco, Oregon. *Tectonics* 9 (5), 983–1014. doi:10.1029/TC009i005p00983
- Kirby, E., Furlong, K. P., Furlong, K. P., von Dassow, W., Worms, K., McKenzie, K., et al. (2020). Does Topography along the Cascadia Forearc Reflect Permanent Deformation of North America? *GSA Connects* 2020: Paper No. 240-3. *Geol. Soc. America Abstr. Programs* 52, 6. doi:10.1130/abs/2020AM-357618
- Kirby, E., McKenzie, K. A., McKenzie, K. A., Furlong, K., and Hefner, W. (2021). Geomorphic Fingerprints of Active Faults in the Southern Cascadia Forearc and Their Geodynamic Significance. *GSA Connects* 2021, Portland, Oregon: Paper No. 30-3. *Geol. Soc. America Abstr. Programs* 53, 6. doi:10.1130/abs/2021AM-370126
- Kirby, E., and Whipple, K. (2001). Quantifying Differential Rock-Uplift Rates via Stream Profile Analysis. *Geol* 29 (5), 415–418. doi:10.1130/0091-7613(2001)029<0415:QDRURV>2.0.CO;2
- Kirby, E., and Whipple, K. X. (2012). Expression of Active Tectonics in Erosional Landscapes. *J. Struct. Geology.* 44, 54–75. doi:10.1016/j.jsg.2012.07.009
- Li, S., Wang, K., Wang, Y., Jiang, Y., and Dosso, S. E. (2018). Geodetically Inferred Locking State of the Cascadia Megathrust Based on a Viscoelastic Earth Model. *J. Geophys. Res. Solid Earth* 123 (9), 8056–8072. doi:10.1029/2018JB015620
- Lock, J., Kelsey, H., Furlong, K., and Woolace, A. (2006). Late Neogene and Quaternary Landscape Evolution of the Northern California Coast Ranges: Evidence for Mendocino Triple junction Tectonics. *Geol. Soc. America Bull.* 118 (9/10), 1232–1246. doi:10.1130/B25885.1
- McCaffrey, R., King, R. W., Payne, S. J., and Lancaster, M. (2013). Active Tectonics of Northwestern U.S. Inferred from GPS-Derived Surface Velocities. *J. Geophys. Res. Solid Earth* 118 (2), 709–723. doi:10.1029/2012JB009473
- McCaffrey, R., Long, M. D., Goldfinger, C., Zwick, P. C., Nabelek, J. L., Johnson, C. K., et al. (2000). Rotation and Plate Locking at the Southern Cascadia Subduction Zone. *Geophys. Res. Lett.* 27 (19), 3117–3120. doi:10.1029/2000GL011768
- McCaffrey, R., Qamar, A. I., King, R. W., Wells, R., Khazaradze, G., Williams, C. A., et al. (2007). Fault Locking, Block Rotation and Crustal Deformation in the Pacific Northwest. *Geophys. J. Int.* 169 (3), 1315–1340. doi:10.1111/j.1365-246X.2007.03371.x
- McCrory, P. A. (2000). Upper Plate Contraction north of the Migrating Mendocino Triple junction, Northern California: Implications for Partitioning of Strain. *Tectonics* 19 (6), 1144–1160. doi:10.1029/1999TC001177
- McCrory, P. A., and Wilson, D. S. (2013). A Kinematic Model for the Formation of the Siletz-Crescent Forearc Terrane by Capture of Coherent Fragments of the Farallon and Resurrection Plates. *Tectonics* 32 (3), 718–736. doi:10.1002/tect.20045
- McKenzie, K. A., Furlong, K. P., and Herman, M. W. (2022). Regional and Local Patterns of Upper-Plate Deformation in Cascadia: the Importance of the Down-Dip Extent of Locking Relative to Upper-Plate Strength Contrasts. *Tectonics.* doi:10.1029/2021TC007062
- McKenzie, K. A., and Furlong, K. P. (2021). Isolating Non-subduction-driven Tectonic Processes in Cascadia. *Geosci. Lett.* 8, 10. doi:10.1186/s40562-021-00181-z
- McQuarrie, N., and Wernicke, B. P. (2005). An Animated Tectonic Reconstruction of Southwestern North America since 36 Ma. *Geosphere* 1 (3), 147–172. doi:10.1130/GES00016.1
- Melnick, D., Bookhagen, B., Echtler, H. P., and Strecker, M. R. (2006). Coastal Deformation and Great Subduction Earthquakes, Isla Santa Maria, Chile (37 S). *Geol. Soc. America Bull.* 118 (11-12), 1463–1480. doi:10.1130/B25865.1
- Meltzer, A. J., Sieh, K., Abrams, M., Agnew, D. C., Hudnut, K. W., Avouac, J.-P., et al. (2006). Uplift and Subsidence Associated with the Great Aceh-Andaman Earthquake of 2004. *J. Geophys. Res.* 111 (B2), a–n. doi:10.1029/2005JB003891
- Muhs, D. R., Rockwell, T. K., and Kennedy, G. L. (1992). Late Quaternary Uplift Rates of Marine Terraces on the Pacific Coast of North America, Southern Oregon to Baja California Sur. *Quat. Int.* 15-16, 121–133. doi:10.1016/1040-6182(92)90041-Y
- Padgett, J. S., Kelsey, H. M., and Lamphear, D. (2019). Upper-plate Deformation of Late Pleistocene marine Terraces in the Trinidad, California, Coastal Area, Southern Cascadia Subduction Zone. *Geosphere* 15 (4), 1323–1341. doi:10.1130/GES02032.1
- Piotraschke, R., Cashman, S. M., Furlong, K. P., Kamp, P. J. J., Danišik, M., and Xu, G. (2015). Unroofing the Klamath-Blame it on Siletzia? *Lithosphere* 7 (4), 427–440. doi:10.1130/L418.1
- Plattner, C., Malservisi, R., Furlong, K. P., and Govers, R. (2010). Development of the Eastern California Shear Zone - Walker Lane belt: The Effects of Microplate Motion and Pre-existing Weakness in the Basin and Range. *Tectonophysics* 485, 78–84. doi:10.1016/j.tecto.2009.11.021
- Ramirez-Herrera, M. T., Gaidzik, K., Forman, S., Kostoglodov, V., Bürgmann, R., and Johnson, C. W. (2018). Relating the Long-Term and Short-Term Vertical Deformation across a Transect of the Forearc in the central Mexican Subduction Zone. *Geosphere* 14 (2), 419–439. doi:10.1130/GES01446.1
- Rohr, K. M. M., Furlong, K. P., and Riedel, M. (2018). Initiation of Strike-Slip Faults, Serpentinization, and Methane: The Nootka Fault Zone, the Juan de

- Fuca-Explorer Plate Boundary. *Geochem. Geophys. Geosyst.* 19 (11), 4290–4312. doi:10.1029/2018GC007851
- Saillard, M., Audin, L., Rousset, B., Avouac, J.-P., Chlieh, M., Hall, S. R., et al. (2017). From the Seismic Cycle to Long-Term Deformation: Linking Seismic Coupling and Quaternary Coastal Geomorphology along the Andean Megathrust. *Tectonics* 36 (2), 241–256. doi:10.1002/2016TC004156
- Savage, J. C., Svarc, J. L., Prescott, W. H., and Murray, M. H. (2000). Deformation across the Forearc of the Cascadia Subduction Zone at Cape Blanco, Oregon. *J. Geophys. Res.* 105 (B2), 3095–3102. doi:10.1029/1999JB900392
- Schmalzle, G. M., McCaffrey, R., and Creager, K. C. (2014). Central Cascadia Subduction Zone Creep. *Geochem. Geophys. Geosyst.* 15 (4), 1515–1532. doi:10.1002/2013GC005172
- Schmidt, W. L., and Platt, J. P. (2018). Subduction, Accretion, and Exhumation of Coherent Franciscan Blueschist-Facies Rocks, Northern Coast Ranges, California. *Lithosphere* 10 (2), 301–326. doi:10.1130/L697.1
- Schwanghart, W., and Scherler, D. (2014). Short Communication: TopoToolbox 2 - MATLAB-Based Software for Topographic Analysis and Modeling in Earth Surface Sciences. *Earth Surf. Dynam.* 2, 1–7. doi:10.5194/esurf-2-1-2014
- Unruh, J., Humphrey, J., and Barron, A. (2003). Transtensional Model for the Sierra Nevada Frontal Fault System, Eastern California. *GeolCO* 31 (4), 3272–3330. doi:10.1130/0091-7613(2003)031<0327:TMFTSN>2.0.CO;2
- Unruh, J., and Humphrey, J. (2017). Seismogenic Deformation between the Sierran Microplate and Oregon Coast Block, California, USA. *Geology* 45 (5), 415–418. doi:10.1130/G38696.1
- Von Dassow, W. A., Kirby, E., and Kirby, E. (2017). Geomorphic Evidence for Differential Rock Uplift across the Southern Cascadia Forearc. GSA Annual Meeting 2017, Seattle, Washington: Paper No. 247-12. *Geol. Soc. America Abstr. Programs* 49, 6. doi:10.1130/abs/2017AM-307033
- Wang, T., Wei, S., Shi, X., Qiu, Q., Li, L., Peng, D., et al. (2018). The 2016 Kaikōura Earthquake: Simultaneous Rupture of the Subduction Interface and Overlying Faults. *Earth Planet. Sci. Lett.* 482, 44–51. doi:10.1016/j.epsl.2017.10.056
- Wells, R. E., Weaver, C. S., and Blakely, R. J. (1998). Fore-arc Migration in Cascadia and its Neotectonic Significance. *Geol* 26 (8), 759–762. doi:10.1130/0091-7613(1998)026<0759:FAMICA>2.3.CO;2
- Whipple, K. X., and Tucker, G. E. (1999). Dynamics of the Stream-Power River Incision Model: Implications for Height Limits of Mountain Ranges, Landscape Response Timescales, and Research Needs. *J. Geophys. Res.* 104 (B8), 17661–17674. doi:10.1029/1999JB900120
- Wilson, D. S. (1993). Confidence intervals for motion and deformation of the Juan de Fuca Plate. *J. Geophys. Res.* 98 (B9), 16053–16071. doi:10.1029/93JB01227
- Wobus, C., Whipple, K. X., Kirby, E., Snyder, N., Johnson, J., Spyropolou, K., et al. (20062006). “Tectonics from Topography: Procedures, Promise, and Pitfalls,” in *Tectonics, Climate, and Landscape Evolution. Geological Society of America Special Paper*. Editors S. D. Willett, N. Hovius, M. T. Brandon, and D. M. Fisher, Vol. 398, 55–74. doi:10.1130/2006.2398(04)
- Zandt, G., and Furlong, K. P. (1982). Evolution and Thickness of the Lithosphere beneath Coastal California. *Geol* 10 (7), 376–381. doi:10.1130/0091-7613(1982)10<376:EATOTL>2.0.CO;2
- Zandt, G., and Humphreys, E. (2008). Toroidal Mantle Flow through the Western U.S. Slab Window. *Geol* 36 (4), 295–298. doi:10.1130/G24611A.1

**Conflict of Interest:** The authors declare that the research was conducted in the absence of any commercial or financial relationships that could be construed as a potential conflict of interest.

**Publisher’s Note:** All claims expressed in this article are solely those of the authors and do not necessarily represent those of their affiliated organizations, or those of the publisher, the editors and the reviewers. Any product that may be evaluated in this article, or claim that may be made by its manufacturer, is not guaranteed or endorsed by the publisher.

Copyright © 2022 McKenzie, Furlong and Kirby. This is an open-access article distributed under the terms of the Creative Commons Attribution License (CC BY). The use, distribution or reproduction in other forums is permitted, provided the original author(s) and the copyright owner(s) are credited and that the original publication in this journal is cited, in accordance with accepted academic practice. No use, distribution or reproduction is permitted which does not comply with these terms.